Arab J. Nucl. Sci. Appl., Vol. 55, 4, 161-191 (2022)

ISSN 1110-0451

Arab Journal of Nuclear Sciences and Applications

Web site: ajnsa.journals.ekb.eg

(E S N S A)

Applying Crystal Model on Different Nuclear Systems; Deuteron, Alpha and ^{6}Li as Projectiles

A. Amar*,a, O. Hemeda a, H. Hashim a, A. R. El Sayed b

[a] *Physics Department, Faculty of Science, Tanta University, Tanta, Egypt*

[b] *Engineering Physics and Mathematics Department, Faculty of Engineering, Tanta University, Tanta 31733, Egypt*

ARTICLE INFO

Article history:

Received: 22nd May 2022

Accepted: 6th Sept. 2022

Keywords:

Coupled Reaction Channel (CRC),

Crystal Model (CM),

Distorted Wave Born Approximation (DWBA),

Dynamic Polarization Potential (DPP),

light nuclei ^{6,7}Li,

^{9}Be, and ^{11}B.

ABSTRACT

Alpha elastically scattered by light nuclei ^{6,7}Li, ^{9}Be, and ^{11} B, has been analyzed in the framework of Coupled Reaction Channel (CRC) and crystal Model (CM) folded with Distorted Wave Born Approximation (CM+DWBA) approach. Also, ^{6}Li elastically scattered by ^{12}C at a wide range of energies has been studied with CRC and CM+DWBA. The effect of transfer on the elastic scattering has been studied to extract the spectroscopic amplitudes for ^{6}Li≡α+d, ^{7}Li≡α+t, ^{9}Be≡α+^{5}He, ^{11}B≡α+^{7}Li and ^{12}C≡^{6}Li+^{6}Li configurations from backward angles of the experimental data under consideration. The crystal Model has been applied for deuteron elastically scattered by ^{6}Li and ^{7}Li where CM+DWBA+DPP (Dynamic Polarization Potential) succeeded to reproduce the differential cross sections for the whole range of angles. The obtained analyses from CRC for alpha elastically scattered by light nuclei ^{6,7}Li, ^{9}Be, and ^{11} B were better than those from CM, which leads to the need for developing the CM in the near future. A fair agreement has been observed between applied models and the considered experimental data.

1. INTRODUCTION

In spite of the fact that the exact solution of the two-bound state problem for Coulomb interaction has been obtained, the similar problem in nuclear system for the deuteron is very complicated. It is believed that the nucleon-nucleon interaction is not elementary, which looks like van der Waals forces acting between atoms [1]. the authors of the present study have discussed similar approach for light nuclei up to ^{7}Be namely, the crystal model approach [2-4] .

Many nuclear models have been modified to analyze the experimental data with satisfied behavior which could produce information about interacting nuclei. Elastic scattering has a special position in the nuclear processes and reactions where varieties of information could be obtained from it. Light nuclei tend to form a cluster as in the case of ^{6,7}Li, ^{9,10}Be, ^{10,11}B which present opportunity to study nuclear structure. Many attempts have been done to find out the atomic structure and mechanisms of nuclear reactions as each model has its ability to interpret some mechanisms with shortage in others. There are a lot of ambiguities in the nuclear parameters (optical potential parameters (OMPs), spectroscopic amplitudes (SA), asymptotic normalization coefficient (ANC), and astrophysical S-factor) where many and many models have been applied to overcome such ambiguities including coupled-cluster approach [5-8] and coupled channel scattering [9-12] which have been studied using lattice calculations at crystal lattice range in Fermi scale.

^{6,7}Li, ^{7,9}Be, and ^{10,11}B tend to form clusters which creates a chance to study them using verity of models [2, 13, 14] .The crystalline model [2] was modified to calculate binding energy for light nuclei ^{6,7}Li, ^{7}Be and ^{8}Be. It is one goal of the nuclear physics and astrophysics to discover the mechanism of nuclear reactions and the structure of nucleus [15].

Guatam and Dean Lee used a general method to study nuclear reactions on the crystal lattice. They have applied their model on the lattice including ^{14}C(n, γ)^{15}C as an example of the applicability of their theory by calculating photo-nuclear reaction rates into the lattice [16]. Ulf-G. Meißner has studied the clustering applying ab initio method on the lattice because high binding energy and spin (isospin) saturated for ^{12}C of alpha particles it was used as the core of the research [17]. The nuclear Lattice Simulations method has been used to explain the clustering in lattice without any constrains

Corresponding author: amar.physics@yahoo.com
DOI: 10.21608/ajnsa.2022.140030.1587

which presents this method as benchmark for ab initio calculations using chiral nuclear EFT [15].

Matter nuclear distribution for ^{6}Li, ^{6}He and ^{9}Be has rearranged nuclear density distribution as previously reported [2] to be suitable for studying light nuclei. Binding energy and nuclear density distribution have been calculated for light nuclei depending on alpha as a core of cluster. They choose ^{6}Li, ^{6}He as (α+n+n) and ^{9}Be as α+α+n, where in case of ^{6}Li it was an approximation to take neutron instead of proton in the configuration [2]. Eldyshev et al.[18] have summarized the form of nuclear density distribution of light nuclei in the form of summation of two Gaussians.

The optical model is able to reproduce differential cross section at forward angles with phenomenological treatment for many nuclear systems that is because at backward angles, there is an increase at the differential cross section resulting from phenomenon known as anomalous large angle scattering (ALAS) [19]. Studying alpha elastically scattered by light nuclei gives an opportunity to apply different models to investigate the structure of the interacting nuclei. Alpha elastically scattered by light nuclei is one tool to examine the structure of the nuclei under consideration. The coupled reaction channel (CRC) is the ideal method to survey the whole range of angles where involving the transfer with elastic scattering is one method to extract spectroscopic amplitude for the configuration. The binding energy could also be adjusted from the fitting process of experimental data by changing it to reproduce the differential cross section.

The crystal model approach has been proposed by the present authors to study alpha elastically scattered by light nuclei. The model has succeeded to reproduce differential cross section for alpha elastically scattered $^{6,7}Li$, ^{9}Be and ^{11}B up to 40MeV/N. The study was achieved using alpha as projectile with z=2 and A=4 for alpha elastically scattered by $^{6,7}Li$, ^{9}Be and ^{11}B [20]. The aim of the present study is to achieve the analysis for alpha elastically scattered by $^{6,7}Li$, ^{9}Be and ^{11}B with another approximation for $z = 3,4,5,\ and\ A = 6,7,9,11$. A comparison will also be done for aforementioned systems with Coupled Reaction Channel calculations.

2. MODELING

2.1 Crystal Model

Optical model still applicable and has many modifications for both real and imaginary parts. New potential form for real part of the optical model has been suggested [4, 20] using the crystal model to study alpha particles with light nuclei with the form:

$$V_{CM}(R) = -V_0 \exp[z(\frac{R}{r_0})^2 - A(\frac{R}{r_0})^2] \quad \textbf{(1)}$$

where V_0 has the value in the range 120-180MeV, $z = 3,4,5,\ A = 6,7,9,11\ and\ r_0 = 1.0 - 2fm$ for $^{6,7}Li$, ^{9}Be and ^{11}B respectively. Where z represents number of protons of the target, A is the atomic number of the target and r_0 is the nucleon radius. The first term $z(\frac{R}{r_0})^2$ of equation (1) represents the repulsive force between the protons of the target under consideration and the second term $-A(\frac{R}{r_0})^2$ is the attractive force between all nucleons inside the target nucleus.

For the deuteron elastically scattered by light nuclei, the crystal model has been modified to be taken as:

$$V_{CM}(R) = -V_0 \exp[-A(\frac{R}{r_0})^2] \quad \textbf{(2)}$$

where the repulsive term was removed because the deuteron has only one proton. The effective potential between projectile and target separated by (R) could be depicted in the crystal model (CM) which may be obtained from the non-relativistic Schrödinger equation:

$$H\psi = \left(-\frac{\hbar}{2\mu}\nabla^2 + U(R)\right) = E\psi(R) \quad \textbf{(3)}$$

where μ is the reduced mass of the projectile and target and E is the energy of the relative motion in center of mass system. The analytical expression used for phenomenological optical model in the present work has been taken in the form:

$$U(R) = V_{CM}(R) + iW(R) + V_C(R) \quad \textbf{(4)}$$

where $V_{CM}(R)$ is real part potential, $W(R)$ is the imaginary part, and $V_C(R)$ is the Coulomb part of the potential. The Woods-Saxon form has been chosen for the imaginary part where real part has a semi-microscopic potential which has general form:

$$Wf(R_v, r, a_v) = -W_0\ ((1 + \exp(\frac{r-R_w}{a_w}))^{-1} \quad \textbf{(5)}$$

where the form factor was taken to be Woods-Saxon form:

$$f(R_i, r, a_i) = ((1 + \exp(\frac{r-r_i A_T^{\frac{1}{3}}}{a_i}))^{-1}, i = W \quad \textbf{(6)}$$

2.2 Coupled Reaction Channel (CRC)

It is considered that CRC is an extension of the optical model and it is extensively used to describe the transfer, inelastic scattering and also their effect on the elastic scattering data. The detailed formalism could be obtained in standard texts,[21] . The analysis has been done for only the ground state of the target, so the optical parameters and spectroscopic amplitudes for ground state have been used. The spectroscopic factor was extracted from backward angles of the elastic scattering data. The bound state for the cluster with a core used Woods-Saxon potential with radius R = 1.25 x $A^{1/3}$ (A = 2, 3, 5, and 7) according to the different considered target's cluster structure, the diffusivity of the well was fixed at a=0.65fm, and the potential depth was adjusted to reproduce the binding energy for the cluster. The cluster state quantum numbers for the considered target's cluster structure were determined by the oscillatory energy conservation relation

$G = 2(N-1) + L = \sum_{i=1}^{n} 2(n_i - 1) + l_i$, where n_i, l_i are the quantum numbers of the components of a cluster of nucleons in the harmonic oscillator model, N, L are the cluster quantum numbers, n is the number of nucleons to be transferred, which is equal to 2, 3, 5, and 7 for $\alpha+^{6,7}$Li, ^{9}Be and ^{11}B respectively.

2.3 Dynamic Polarization Potential

The normalization factor of the real part calculated from the folding model for weakly bound nuclei, ^{6,7}Li, ^{9}Be and ^{11}B is found to be less than unity, Nr<1[22] . In the case of alpha elastically scattered by light nuclei, the crystal model potential is decreased, and the required normalization factor for reproducing the experimental data of the systems under consideration has been found to be about 0.5–0.8. In the present analysis, alpha and deuteron elastically scattered by ^{6}Li, ^{7}Li, ^{9}Be and ^{11}B using real CM+DWBA potential, the Nr should be reduced by about 20% to well reproduce the experimental data. To solve the reduction problem in the CM+DWBA potential, non-renormalized real CM+DWBA+DPP potential with (Nr=1) has been applied to the systems under consideration. The DPP is taken as a complex surface potential Upol=Vpol+iWpol, with a repulsive real part Vpol [23]: .

$$\Delta U_{pol.} = V_{pol.} + iW_{pol.} \quad \textbf{(7)}$$

Where $V_{pol}(R) = -V_{pol}.\ f(R)$, $W_{pol}(R) = -W_{pol}.f(R)$, and

$$f(R) = \exp\left(\frac{R-R_{pol}}{a_{pol}}\right) / \left[1 + \exp\left(\frac{R-R_{pol}}{a_{pol}}\right)\right]^2 \quad \textbf{(8)}$$

where $R_{pol} = r_{pol}A_t^{1/3}$

Thus,

$$V_{pol}(R) = -V_{pol}f(R) = -V_{pol}\exp\left(\frac{R-R_{pol}}{a_{pol}}\right) / \left[1 + \exp\left(\frac{R-R_{pol}}{a_{pol}}\right)\right]^2, \quad \textbf{(9)}$$

The form of the total optical potential can be written as:

$$U(R) = V_{CM}(R) + iW(R) + V_C(R) + V_{pol}(R) \quad \textbf{(10)}$$

3. RESULTS AND DISCUSSION

3.1 Alpha Elastically scattered by ^{6}Li

Studying the protons, deuterons, and alpha elastically scattered by ^{6}Li have been widely used in the nuclear physics and astrophysical studies. Several studies have been achieved for alpha elastically scattered by ^{6}Li at energies 2.5 to 4.5 MeV [24], 12 to 18.5 MeV [25], 29.4 MeV [26], 36.6 MeV [27], 35 to 45 MeV [28], 50 MeV [29-31], 59 MeV [32], 104 MeV [33], and 166 MeV [34]

Alpha elastically scattered by ^{6}Li is one choice to study its structure where deuteron and triton, also, could be used for the same purpose. The optical model was used to analyze experimental data at forward angles where at backward angles Distorted Wave Born Approximation (DWBA) was applied to reproduce differential cross sections. Optical potential parameters have been obtained on the region where the potential scattering is dominant by the comparison of theoretical and experimental cross sections in the region of forward angles θ≤90°. The whole range of angles for alpha elastically scattered by ^{6}Li have been investigated with the coupled reaction channel method that is by involving inelastic scattering to elastic with deuteron transfer at backward angles as shown in Fig. (1). The cluster suggested for ^{6}Li appears at backward angles of elastic scattering if the complementary of the nucleus core is used as a projectile. For example, alpha is a complementary of deuteron (as a core) in case of ^{6}Li. Global optical potential parameters for A<12 for interaction of alpha with a nucleus are not available to date where the compilation of phenomenological optical-model parameters was available since 50 years ago [35]. Also, global optical potential parameters have been achieved for ^{12}C up to ^{208}Pb [36] and 20 ≤ A ≤ 209 at incident energies below 386MeV [37]. One step transfer has been applied to alpha elastically scattered by ^{6}Li, which reproduces the differential cross section in satisfied behavior where negligible role has been observed from two-step transfer especially at higher energies [38]. The coupling between the ground state of ^{6}Li nucleus (1^+) and first excited state (E_x=2.186 MeV, 3^+) for both channels was calculated with the collective form factor of the rotational model for quadrupole transitions (λ = 2):

$$V_\lambda(r) = -\frac{\delta_\lambda}{\sqrt{4\pi}}\frac{dU(r)}{dr} \quad \textbf{(11)}$$

where δ_λ is a multipole deformation length. Reorientation effects defined by matrix elements $\langle EJ^\pi|V_2|EJ^\pi\rangle$ were also calculated for quadrupole transitions. The coupling scheme is shown in Fig. (2). The crystal model has been applied to alpha elastically scattered by ^{6}Li at E_{α}=18, 29.4, 36.6, 50.5, 59, 104 and 166MeV. The crystal model is considered as folding model with normalization parameter as presented into Table (2). The normalization factor obtained from crystal model is close to that obtained from double folding [39-41].For the crystal model approach, DWBA has been involved to study the backward angles in addition to obtain spectroscopic information from deuteron transfer at backward angles. The real part was taken from the crystal model where imaginary part was in the Woods-Saxon form. The imaginary potential depth has been modified from CRC method to obtain the best fit of the considered experimental data as presented in Table (2). At low energy E_{α}=18MeV, CM+DWBA succeeded to reproduce differential cross section even better than that is from CRC as shown in Fig. (1), where, strong coupling channel has been observed at such energy. With increasing projectile energy new channels open which produces a sharp increase in the imaginary part of the potential. Threshold anomaly has been remarked in [38], at 18MeV where the authors discussed the absence of such scattering process at loosely bound nucleus such as $^{6}\mathrm{Li} \rightarrow \alpha + d$ which has a threshold for the breakup process equal 1.47 MeV. The optical potential parameters taken from [38],succeeded to reproduce differential cross sections from 18 to 50MeV (Fig. 2). There is an abnormal behavior at E_{α}= 36MeV for both models drawn in Fig. (2), where a sharp increase in differential cross section has been observed. A sudden increase in the imaginary potential depth has been observed at 29.4 and 36.6MeV in case of CRC which indicates a possibility of manifestation some threshold anomaly. Threshold anomaly has been observed only at 36.6MeV when CM+DWBA has been applied. At 45, 50, 59MeV, poor analysis has been obtained at intermediate angles by applying CM+DWBA where better analysis was at 104 and 166MeV.

The value of σ_R can be calculated from the transmission coefficients T_l corresponding to the l-wave elastic scattering matrix elements S_l [42] :

$$\sigma_R = \pi\lambda^2 \sum_l (2l+1)\, T_l \qquad \textbf{(12)}$$

Where:

$$T_l = 1 - |S_l|^2 \qquad \textbf{(13)}$$

The calculated cross sections for alpha elastically scattered by ^{6,7}Li, ^{9}Be and ^{11}B were found to be in agreement with the predictions obtained in the previous study [42] where the best agreement with the experimental data values is obtained with the deep potential assumption given in Table (2). Cluster quantum numbers for the overlap used in our calculations are listed in Table (1).

Table (1): N, L, S and J for the overlap used in our calculations

T Overlap	*N* No. of nodes	*L*	*S*	*J=L+S*	B.E MeV
$\langle ^{6}\mathrm{Li} \mid \alpha \rangle$	2	0	1	1	1.447
$\langle ^{7}\mathrm{Li} \mid \alpha \rangle$	2	1	0.50	1.50	2.467
$\langle ^{9}\mathrm{Be} \mid \alpha \rangle$	3	1	0.50	1.50	2.467
$\langle ^{11}\mathrm{B} \mid \alpha \rangle$	4	1	0.50	1.50	8.665

CM+DWBA enhanced the fitting of the experimental data at 18MeV, 29.4MeV and 36.6MeV for alpha elastically scattered by ^{6}Li as shown in Fig.(1). Elastic scattering, deuteron transfer with elastic scattering and inelastic scattering has been involved in the CRC calculations during the analysis leads to observable enhancement on the experimental data analysis at forward angles [22]. The extracted spectroscopic amplitudes using CM+DWBA is slightly energy dependent. Reliable spectroscopic amplitudes have been extracted applying CM+DWBA for alpha elastically scattered by ^{6}Li because elastic and deuteron transfer with elastic scattering have been taken into account. By energy increasing, the value of spectroscopic amplitude decreases to about 50% in comparison with theory 1.06 for $^{6}\mathrm{Li} \equiv d + \alpha$ configuration [43] .

In the present analysis for α+^{6}Li, α+^{7}Li, α+^{9}Be and α+^{11}B systems using real CM+DWBA potential, the N_r should be reduced by about 20% to well reproduce the experimental data. Dynamic polarization potential (DPP) has been examined to alpha elastically scattered by ^{6}Li as the normalization factor is less than unity. DPP has been applied to all energies under consideration where poor analysis has been obtained at lower energies where at such low energies, the compound system is dominant and elastic scattering is not completely responsible for the calculated differential cross section. The analysis of the considered experimental data has been improved when DPP has been involved during the fitting process at higher energies as shown in Fig.(1). The coupling scheme used in calculations of alpha elastic scattering on ^{6}Li, ^{7}Li, ^{9}Be, and ^{11}B nuclei using the coupled reaction channels (CRC) method was taken from a previous work[22]. The energy dependence of all studied parameters presented in Table (2) are shown in Fig. (2). As shown in Fig.(1), there is a discrepancy between the experimental points in the angular distributions and their corresponding theoretical calculations; especially those of the CM+DWBA, at some scattering angles for some interacting particles where inelastic scattering does not involved at such analysis.

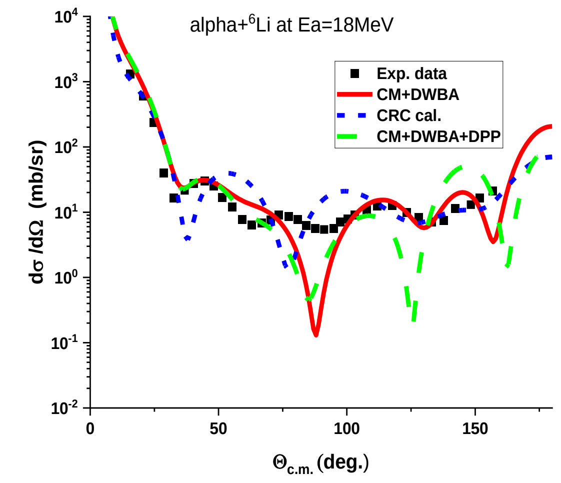
alpha+6Li at Ea=18MeV
Exp. data
CM+DWBA
CRC cal.
CM+DWBA+DPP
dσ /dΩ (mb/sr)
Θc.m. (deg.)

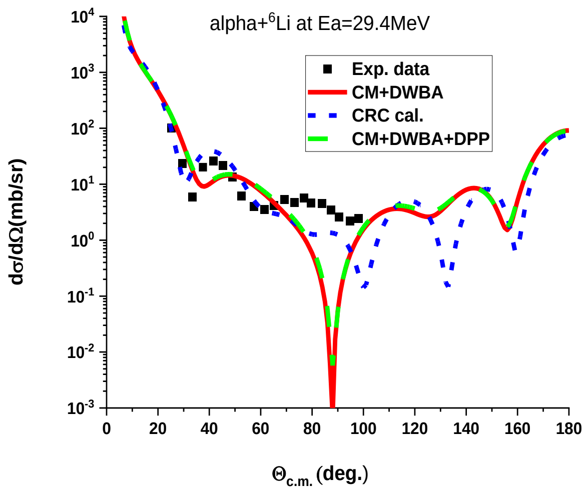
alpha+6Li at Ea=29.4MeV
Exp. data
CM+DWBA
CRC cal.
CM+DWBA+DPP
dσ/dΩ(mb/sr)
Θc.m. (deg.)

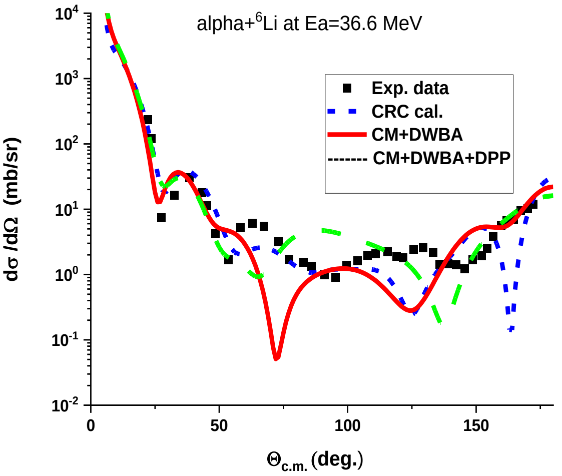
alpha+6Li at Ea=36.6 MeV
Exp. data
CRC cal.
CM+DWBA
CM+DWBA+DPP
dσ /dΩ (mb/sr)
Θc.m. (deg.)

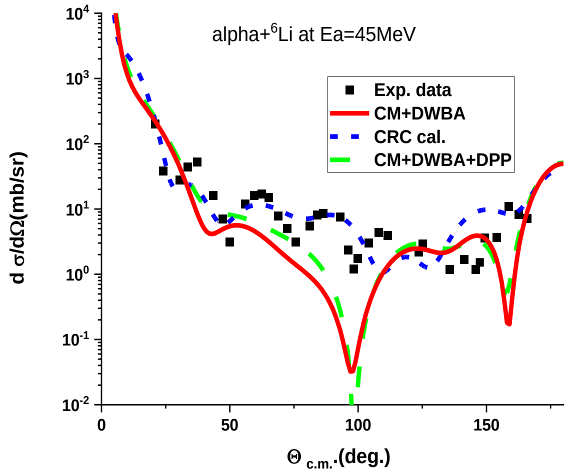
alpha+6Li at Ea=45MeV
Exp. data
CM+DWBA
CRC cal.
CM+DWBA+DPP
d σ/dΩ(mb/sr)
Θ c.m..(deg.)

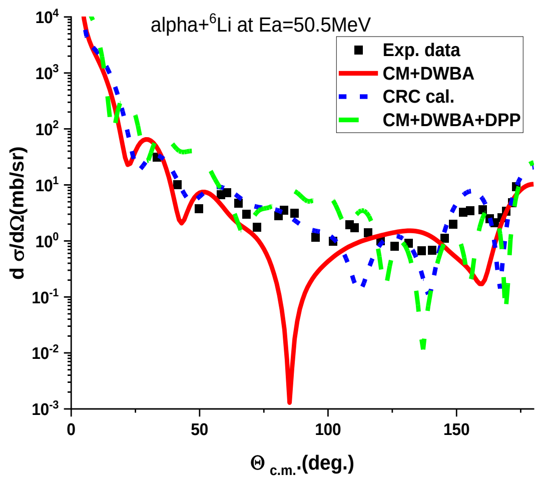
alpha+6Li at Ea=50.5MeV
Exp. data
CM+DWBA
CRC cal.
CM+DWBA+DPP
d σ/dΩ(mb/sr)
Θ c.m..(deg.)

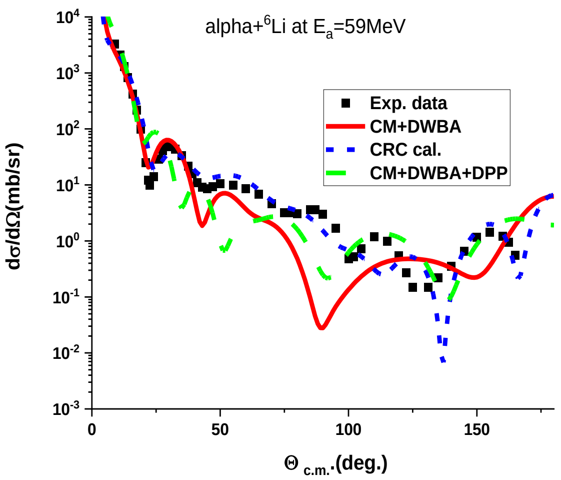
alpha+6Li at Ea=59MeV
Exp. data
CM+DWBA
CRC cal.
CM+DWBA+DPP
dσ/dΩ(mb/sr)
Θ c.m..(deg.)

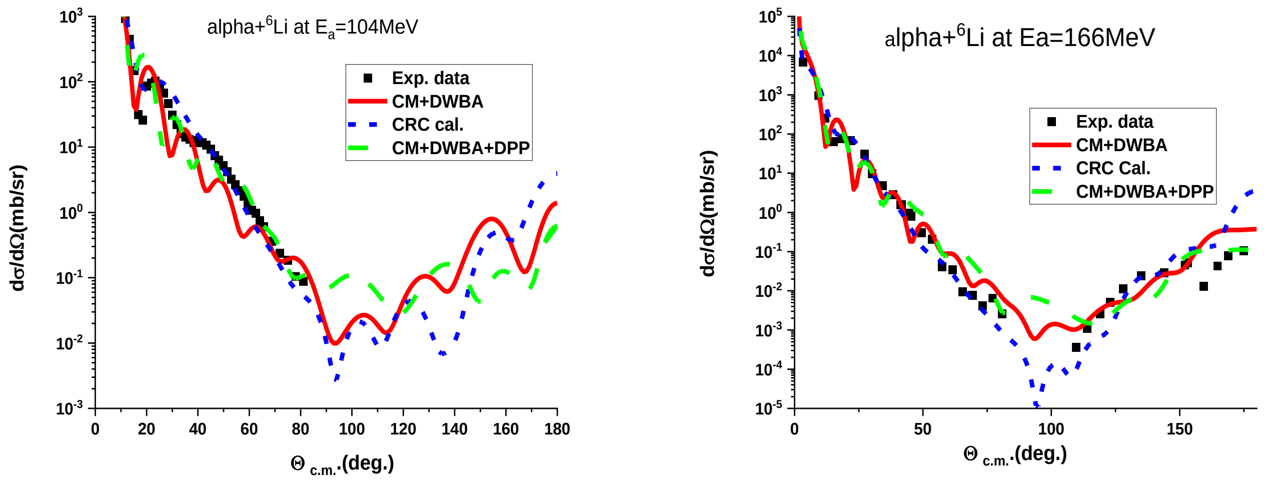

Fig. (1): Angular distribution for alpha elastically scattered by ^{6}Li, square dots represents experimental data, short dot lines (blue) represent CRC calculations, red lines represent calculated results from crystal model (CM+DWBA) and green lines are the CM+DWBA+DPP potential.

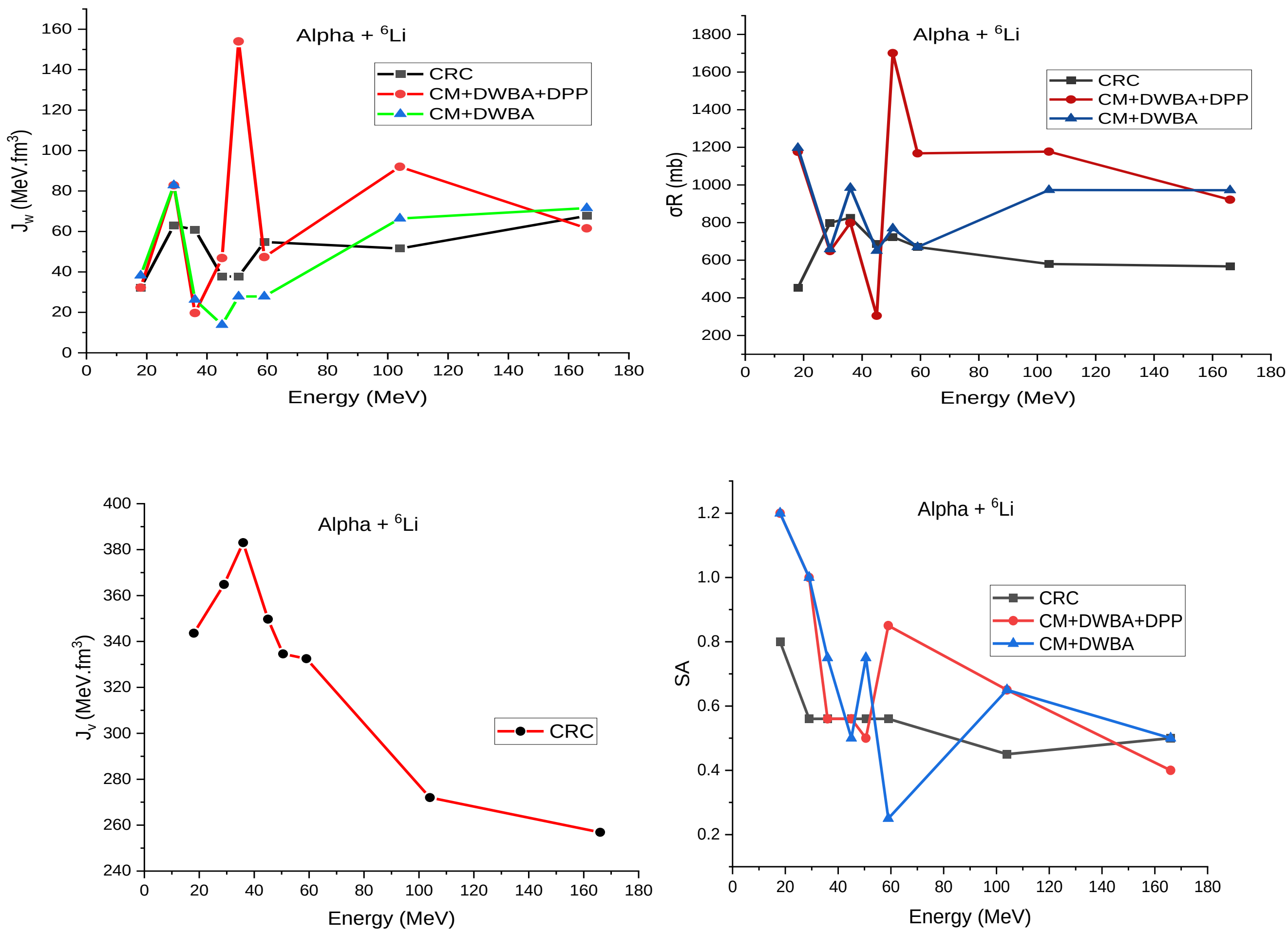

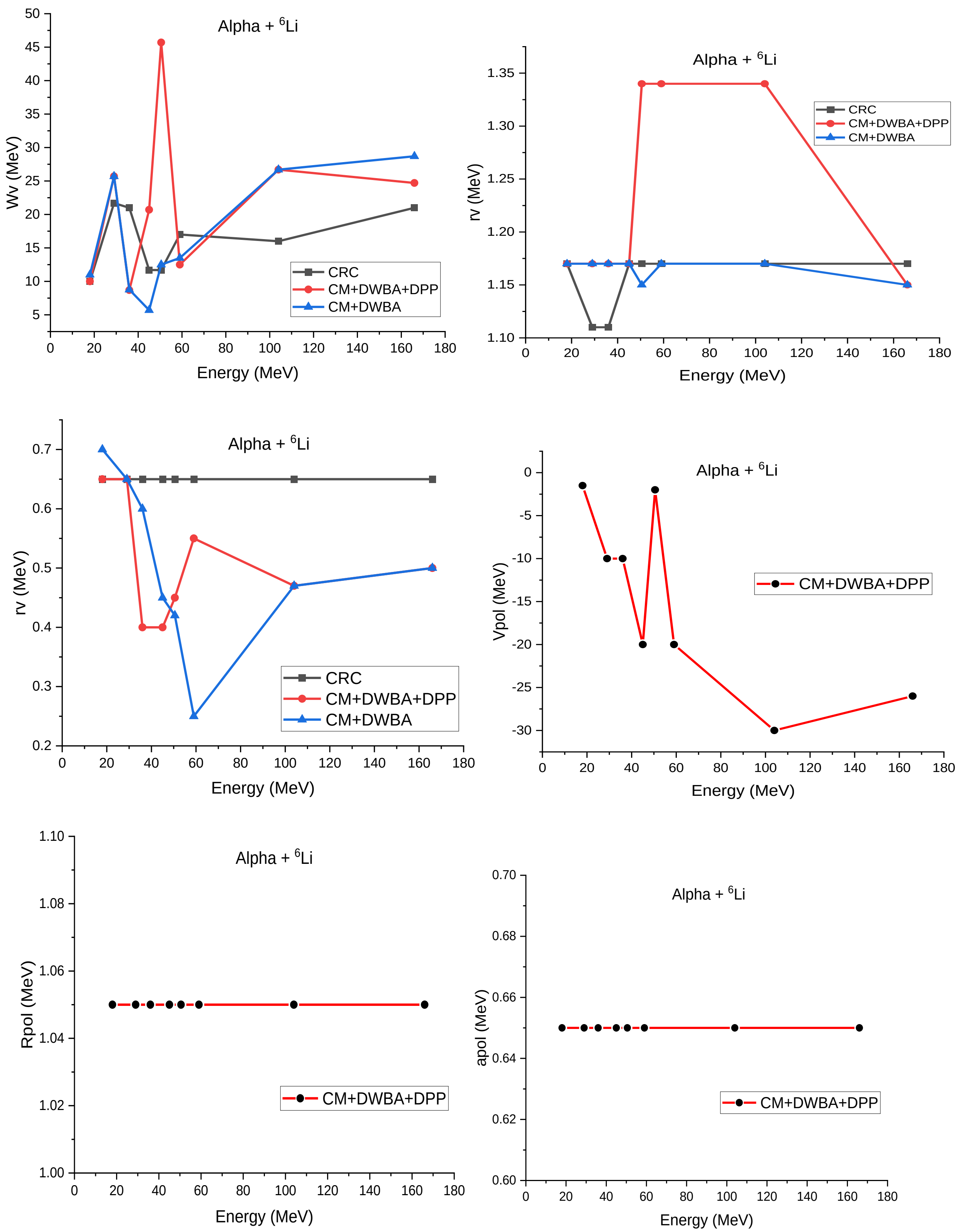

Fig. (2): Energy dependence of the total cross-section, real and imaginary potentials, DPP parameters, SA, radius, diffuseness, and volume integrals for the real and imaginary parts of the CM+DWBA and CM+DWBA+DPP potentials per nucleon pair for α-particles elastically scattered by ^{6}Li

Table (2): The parameters obtained for alpha elastically scattering by ^{6}Li with fixed r_c at 1.3 fm for calculations where (CM) is crystal model calculations

Eα MeV	Model	V0, MeV	r0, fm	a0, fm	Wv, MeV	rv, fm	av, fm	Vpol MeV	Rpol fm	apol fm	Jv MeV.fm3	Jw MeV.fm3	SA	σR , mb	*Ref.*
18.0	CRC	113.5	1.15	0.78	10.0	1.17	0.65				343.6	32.245	0.80	453.0	[22]
	CM+DWBA+DPP	Nr=1.00			10.0	1.17	0.65	-1.50	1.05	0.65		32.245	1.20	1176	p.w.
	CM+DWBA	Nr=0.80			11.0	1.17	0.70					38.188	1.20	1197	p.w.
29.0	CRC	126.0	1.15	0.78	21.7	1.11	0.65				364.8	62.932	0.56	798.3	[22]
	CM+DWBA+DPP	Nr=1.00			25.7	1.17	0.65	-10.0	1.05	0.65		82.869	1.00	648.6	p.w.
	CM+DWBA	Nr=0.75			25.7	1.17	0.65					82.869	1.0	658.3	p.w.
36.0	CRC	120.00	1.15	0.78	21.0	1.11	0.65				383.0	60.902	0.56	826.1	[22]
	CM+DWBA+DPP	Nr=1.00			08.7	1.17	0.40	-10.0	1.05	0.65		19.689	0.56	798.3	p.w.
	CM+DWBA	Nr=0.56			8.77	1.17	0.60					26.271	0.75	984.8	p.w.
45.0	CRC	115.00	1.15	0.78	11.7	1.17	0.65				349.7	37.726	0.56	686.2	[22]
	CM+DWBA+DPP	Nr=1.00			20.7	1.17	0.40	-20.0	1.05	0.65		46.847	0.56	304.5	p.w.
	CM+DWBA	Nr=0.56			05.7	1.17	0.45					13.787	0.50	649.5	p.w.
50.5	CRC	115.00	1.15	0.78	11.7	1.17	0.65				334.6	37.726	0.56	723.6	[22]
	CM+DWBA+DPP	Nr=1.00			45.7	1.34	0.45	-2.0	1.05	0.65		153.964	0.50	1701	p.w.
	CM+DWBA	Nr=0.50			12.5	1.15	0.42					27.845	0.75	769.2	p.w.
59.0	CRC	110.00	1.15	0.78	17.0	1.17	0.65				332.5	54.816	0.56	670.2	[22]
	CM+DWBA+DPP	Nr=1.00			12.5	1.34	0.55	-20.0	1.05	0.65		47.355	0.85	1168	p.w.
	CM+DWBA	Nr=0.10			13.50	1.170	0.25					27.845	0.25	670.2	p.w.
104	CRC	90.00	1.15	0.78	16.0	1.17	0.65				272.0	51.592	0.45	579.6	[22]
	CM+DWBA+DPP	Nr=1.00			26.7	1.34	0.47	-30.0	1.05	0.65		92.013	0.65	1177	p.w.
	CM+DWBA	Nr=0.72			26.7	1.17	0.47					66.381	0.65	973.2	p.w.
166	CRC	85.00	1.15	0.78	21.0	1.17	0.65				256.9	67.714	0.50	567.1	[22]
	CM+DWBA+DPP	Nr=1.00			24.7	1.15	0.50	-26.0	1.05	0.65		61.566	0.40	921.7	p.w.
	CM+DWBA	Nr=0.75			28.7	1.15	0.50					71.536	0.50	971.8	p.w.

3.2 Alpha Elastically scattered by ^{7}Li

The CRC alpha elastically scattered by ^{7}Li analysis was carried out by optimizing four free parameters, two for real WS potential (V_o, a_o) and two for imaginary WS potential (W_v, a_v) where the radii $r_o = 1.281\, fm$ and $r_v = 1.34\, fm$ were fixed are given in Table (3). The coupling between the ground state of ^{7}Li nucleus (3/2$^-$) and first excited state (E_x=0.477MeV, 1/2$^-$) for both channels was calculated with the collective form factor of the rotational model for quadrupole transitions from Eq. (11). The optical model parameters and spectroscopic amplitudes for ground state have been used for first excited state as approximation.

Threshold anomaly has been observed at E_α=50.5MeV which is detected from the extreme increase in the imaginary potential depth by CRC method. The threshold of ^{6}Li is lower than ^{7}Li delays threshold anomaly on ^{7}Li to higher energies up to 50.5MeV instead of 29 and 36MeV in case of ^{6}Li. The coupling scheme used in the present calculations of alpha elastic scattering on ^{7}Li shown in Fig.(3). The comparison between the experimental data for the alpha elastically scattered by ^{7}Li at energies 12-50 MeV [25, 30, 44, 45] and the theoretical calculations within the framework of the CM and CRC using FRESCO code [46] is shown in Fig. (3). CM+DWBA could reproduce differential cross sections at the whole range of angles and energies in fair manner for alpha elastically scattered by ^{7}Li. The break-up of ^{6,7}Li is responsible for the reduction of normalization factor to less unity [47]. Extracted spectroscopic amplitudes from CM+DWBA are higher than those obtained from CRC are given in Table (3). The obtained best fit of the considered experimental data of alpha elastically scattered by ^{7}Li applying CM is better at 12-29MeV than at the higher energy 50MeV. CM+DWBA works well at lower energies than at higher energies as shown in Fig. (3). The energy dependence of all studied parameters presented in Table (3) are shown in Fig. (4). As mentioned in Fig. (1), there is a discrepancy in Fig.(3) between the experimental points in the angular distributions and their corresponding theoretical calculations; especially those of the CM+DWBA, at some scattering angles for some interacting particles and also, inelastic scattering which did not involve at the analysis affected on the fitting especially at intermediate angles. Where the CM works well at forward angles at some cases (see alpha elastically scattered by ^{7}Li at 18MeV).

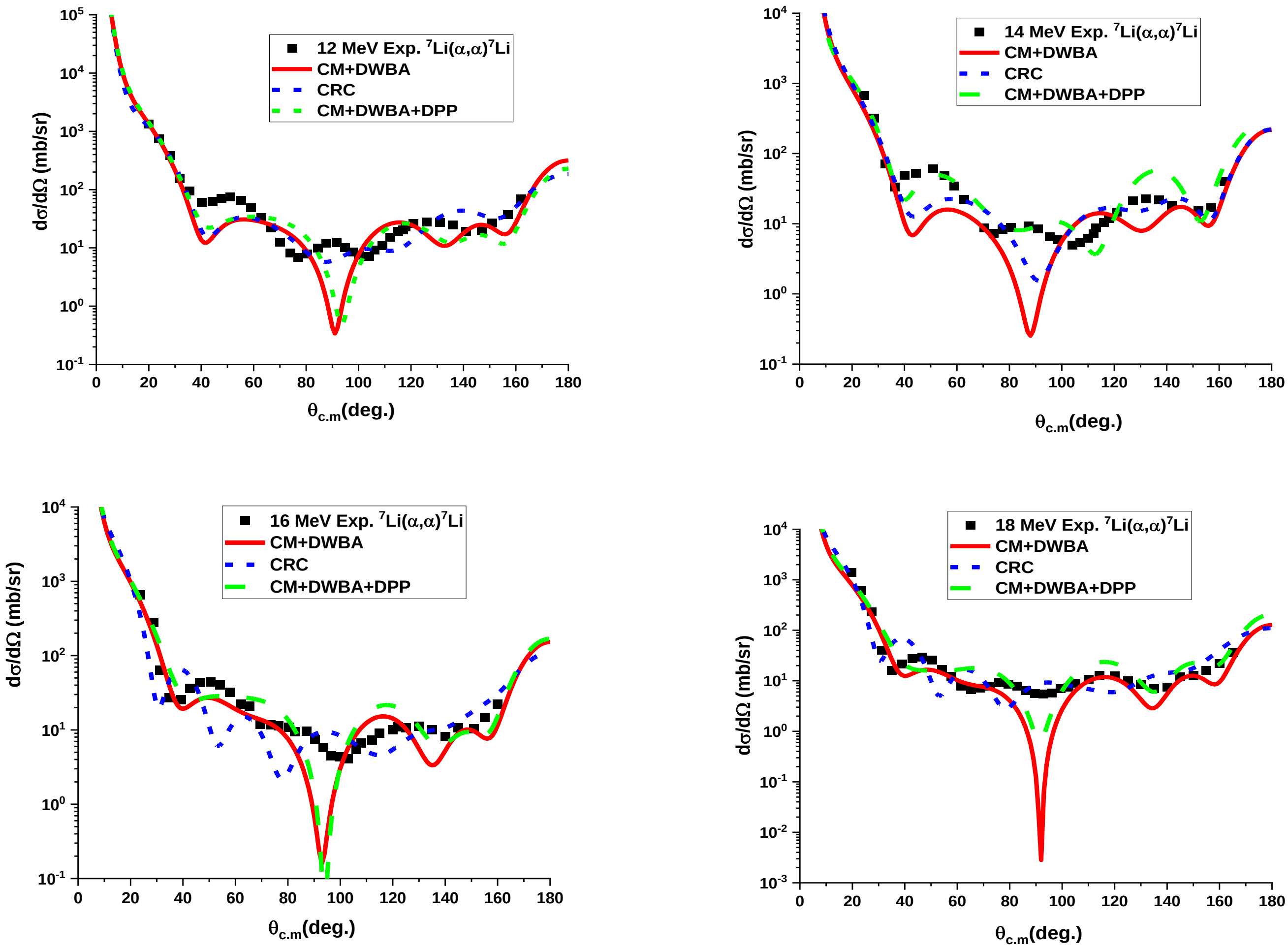

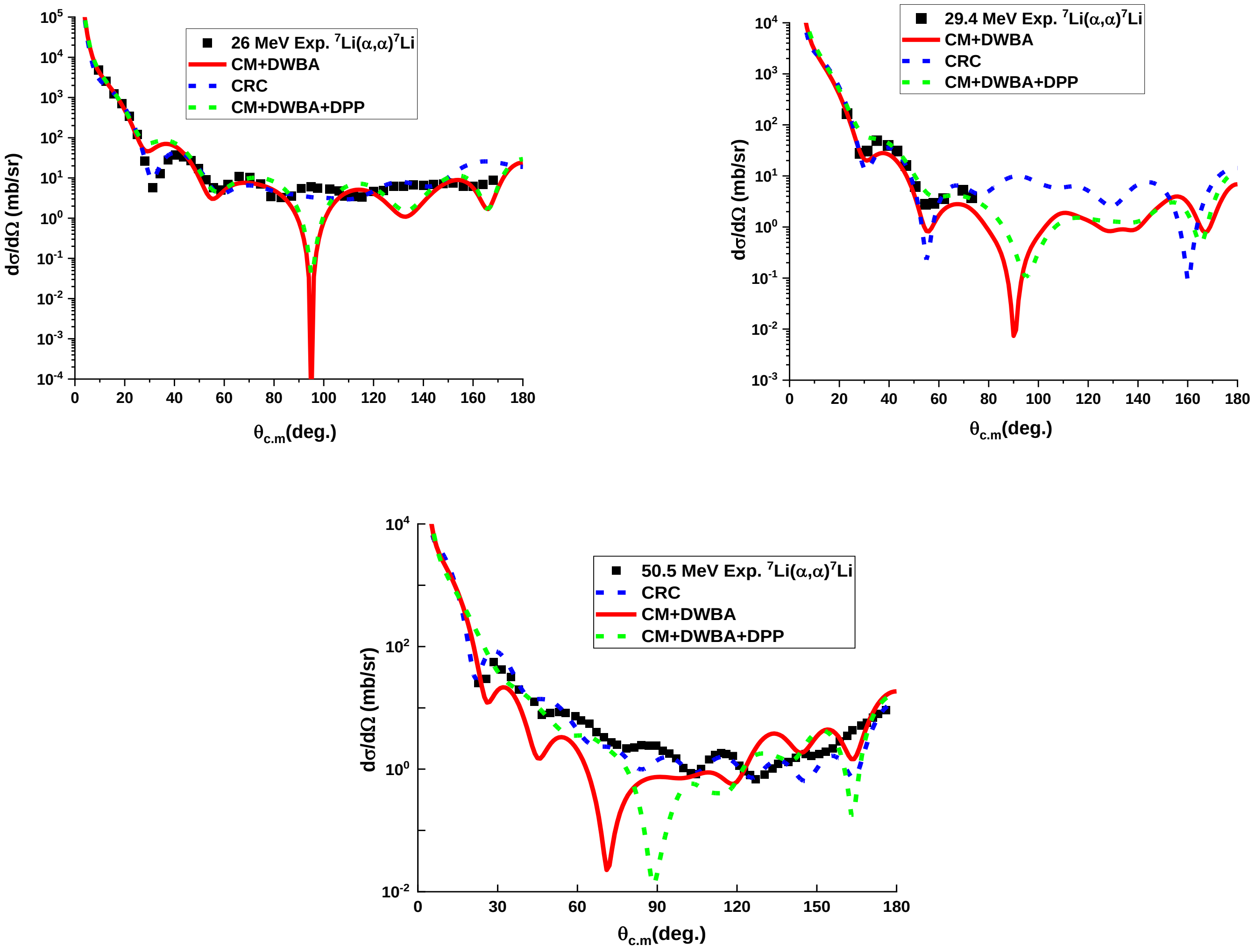

Fig. (3): Angular distribution for alpha elastically scattered by ^{7}Li, square dots represents experimental data, short dot lines (blue) represent CRC calculations and solid lines red lines represent calculated results from crystal model (CM+DWBA) and green lines are the CM+DWBA+DPP potential where experimental data were taken from [25, 30, 44, 45].

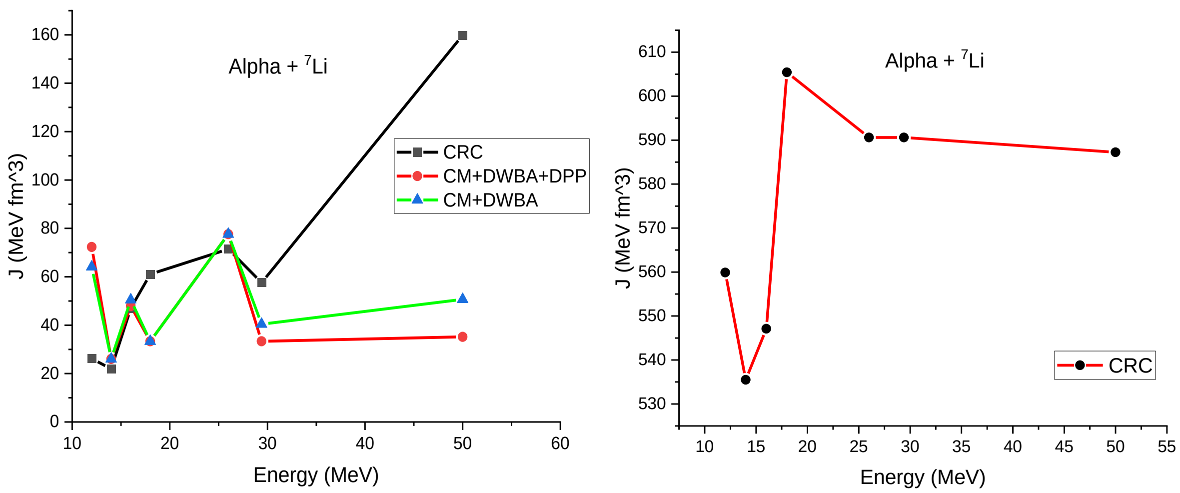

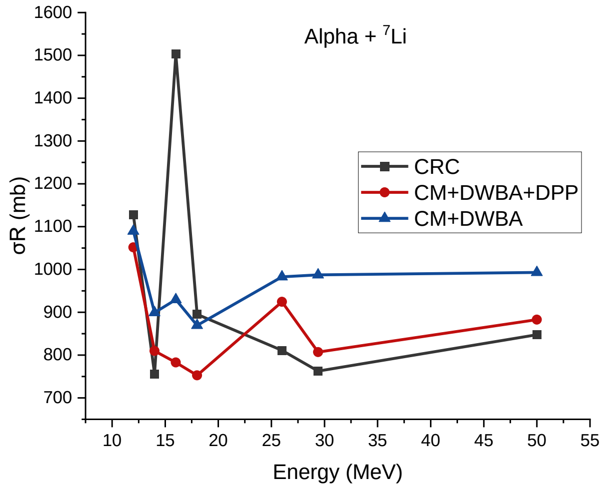
Alpha + ^{7}Li
CRC
CM+DWBA+DPP
CM+DWBA
σR (mb)
Energy (MeV)

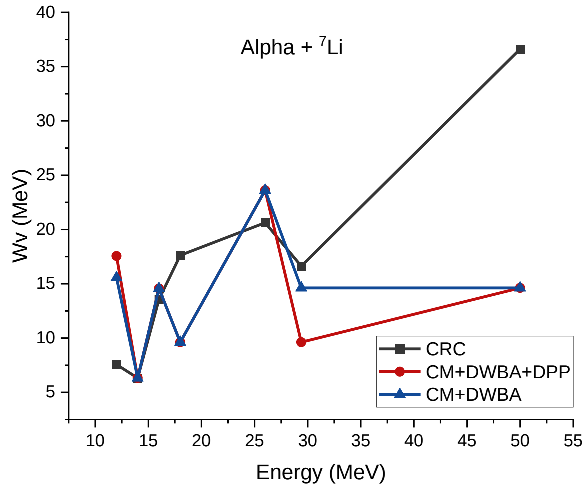
Alpha + ^{7}Li
CRC
CM+DWBA+DPP
CM+DWBA
Wv (MeV)
Energy (MeV)

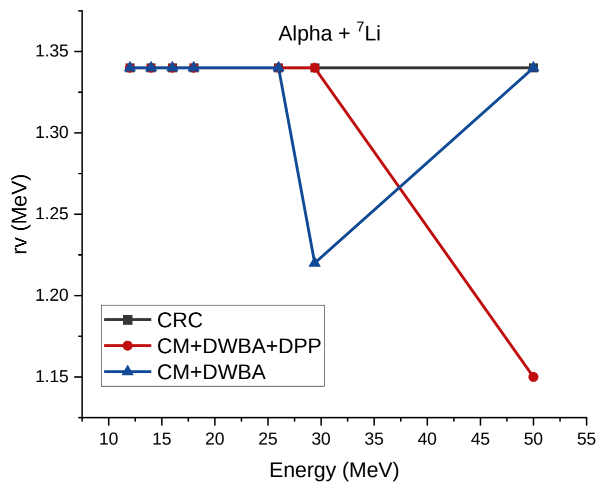
Alpha + ^{7}Li
CRC
CM+DWBA+DPP
CM+DWBA
rv (MeV)
Energy (MeV)

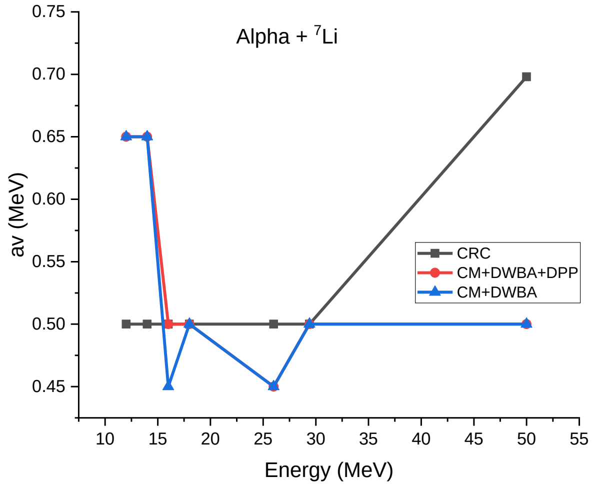
Alpha + ^{7}Li
CRC
CM+DWBA+DPP
CM+DWBA
av (MeV)
Energy (MeV)

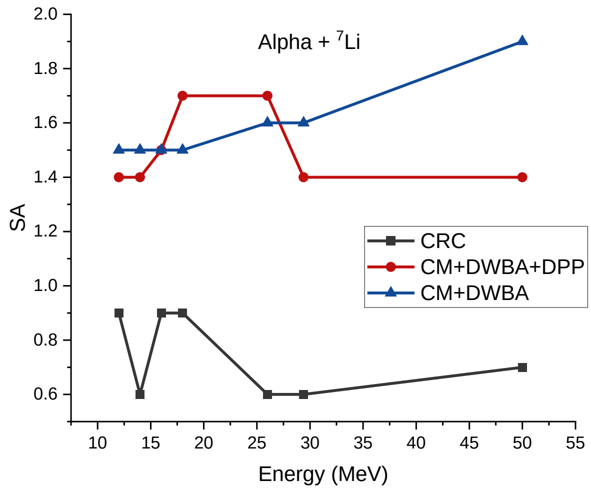
Alpha + ^{7}Li
CRC
CM+DWBA+DPP
CM+DWBA
SA
Energy (MeV)

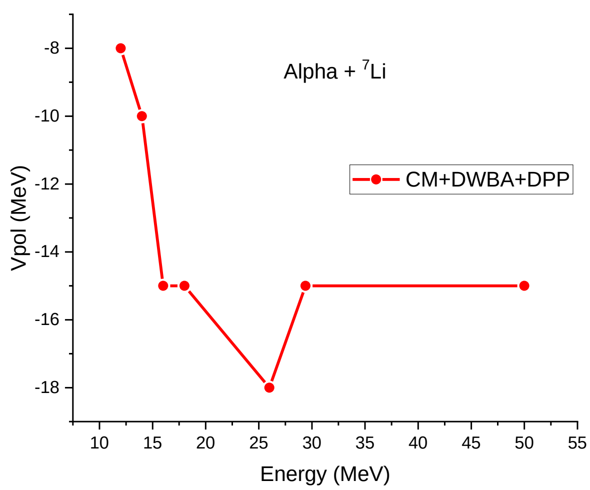
Alpha + ^{7}Li
CM+DWBA+DPP
Vpol (MeV)
Energy (MeV)

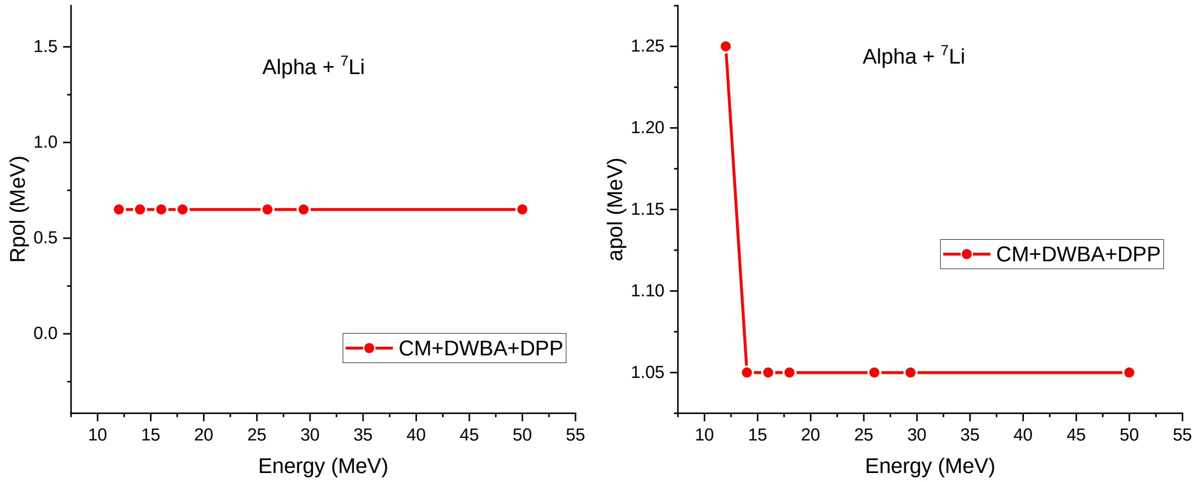

Fig. (4): Energy dependence of the total cross-section, real and imaginary potentials, DPP parameters, SA, radius, diffuseness, and volume integrals for the real and imaginary parts of the CM+DWBA and CM+DWBA+DPP potentials per nucleon pair for α-particles elastically scattered by ^{7}Li

Table (3): The obtained optical parameters for alpha elastically scattering by ^{7}Li with fixed r_c at 1.3 fm for calculations where (CM) is crystal model calculations

E_α MeV	Model	V_0, MeV	r_0, fm	a_0, fm	W_v, MeV	r_v, fm	a_v, fm	$V_{pol.}$	$r_{pol.}$	$a_{pol.}$	J_v MeV.fm^3	J_w MeV.fm^3	SA	σ_R, mb	*Ref.*
12.0	CRC	124.8	1.28	0.79	07.56	1.340	0.5				559.9	26.20	0.9	1127.3	**[22]**
	CM+DWBA+DPP	Nr=0.80			17.56	1.340	0.65	-8.0	1.25	0.65		72.32	1.4	1051.5	
	CM+DWBA	Nr=1.0			15.56	1.340	0.65					64.08	1.5	1089.5	
14.0	CRC	137.8	1.28	0.68	06.32	1.340	0.5				535.5	21.90	0.6	756.30	**[22]**
	CM+DWBA+DPP	Nr=0.80			06.32	1.340	0.65	-10.0	1.05	0.65		26.03	1.40	809.77	
	CM+DWBA	Nr=1.0			06.32	1.340	0.65					26.03	1.50	899.07	
16.0	CRC	175.9	1.28	0.50	13.57	1.340	0.5				547.10	47.03	0.90	1503.0	**[22]**
	CM+DWBA+DPP	Nr=0.80			14.57	1.340	0.45	-15.0	1.05	0.65		47.87	1.50	782.92	
	CM+DWBA	Nr=1.0			14.57	1.340	0.50					50.49	1.50	929.44	
18.0	CRC	132.94	1.28	0.80	17.62	1.34	0.5				605.43	61.06	0.90	895.20	**[22]**
	CM+DWBA+DPP	Nr=0.80			09.62	1.340	0.50	-15.0	1.05	0.65		33.34	1.70	752.76	
	CM+DWBA	Nr=1.0			09.62	1.340	0.50					33.34	1.50	869.36	
26.0	CRC	158.9	1.28	0.64	20.62	1.340	0.50				590.6	71.46	0.60	811.00	**[22]**
	CM+DWBA+DPP	Nr=0.80			23.62	1.340	0.45	-18.0	1.05	0.65		77.61	1.70	924.44	
	CM+DWBA	Nr=1.0			23.62	1.340	0.45					77.61	1.60	982.72	
29.4	CRC	158.9	1.281	0.647	16.62	1.34	0.5				590.6	57.60	0.60	762.55	**[22]**
	CM+DWBA+DPP	Nr=0.80			09.62	1.340	0.50	-15.0	1.05	0.65		33.34	1.40	806.93	
	CM+DWBA	Nr=1.0			14.62	1.22	0.50					40.39	1.60	987.30	
50.0	CRC	141.9	1.28	0.72	36.62	1.34	0.698				587.23	159.79	0.70	847.70	**[22]**
	CM+DWBA+DPP	Nr=0.80			14.62	1.150	0.50	-15.0	1.05	0.65		35.15	1.40	882.93	
	CM+DWBA	Nr=1.0			14.62	1.340	0.50					50.67	1.90	992.90	

3.3 Alpha Elastically scattered by ^{9}Be

The interaction between light-light nuclei has been investigated in [44, 48, 49]. It is thought that light nuclei tend to form clusters as ^{9}Be= (α+^{5}He, d+^{7}Li, t+^{6}Li, and n+^{8}Be). The configuration n+^{8}Be has been thought to have the higher probability than other configurations [50] equal 68.7% where α+^{5}He configuration has only 25.1% from total probability of ^{9}Be cluster configurations. It has been expected that ^{9}Be nucleus exhibit exotic nuclei properties [51-54]. The optical model is able to reproduce forward angles differential cross section where backward angles need sophisticated models.

Many investigations of ^{9}Be structure have been done at Eα=35MeV [55], Eα=65MeV [51], and at E_α=18MeV[56]. ^{9}Be is a weakly bound nucleus resulting from Borromean structure which breaks up into n+α, n+^{8}Be (2α in 10^{-16}sec). ^{9}Be has a rotational band (K^π = 3/2⁻) built on its ground state. $3/2^-$, $5/2^-$ and $7/2^-$ states of ^{9}Be were included into the CRC calculations for inelastic scattering. Inelastic scattering parameters for $^{9}Be(\alpha,\alpha')^{9}Be$ were taken to be $\beta_\lambda R_V$=1.574fm and β_2=0.64 [57] . ^{5}He transfer and inelastic scattering with elastic scattering have been included into CRC calculation on $^{9}Be(\alpha,\alpha)^{9}Be$ and $^{9}Be(\alpha,^{9}Be)\alpha$ for whole range of angles shown in Fig. (5). The sudden increase of imaginary potential depth applying to both the CRC and CM calculations at 29 and 40MeV for alpha elastically scattering by ^{9}Be is a possibility of manifestation of some threshold anomaly. The depth of the imaginary potential part have been justified in case of CM+DWBA from the CRC calculations to reproduce differential cross section for $^{9}Be(\alpha,\alpha)^{9}Be$ and $^{9}Be(\alpha,^{9}Be)\alpha$ at all energies under consideration where experimental data were taken from [48, 49, 58, 59] as shown in Fig. (5). The energy dependence of all studied parameters presented in Table (4) are shown in Fig. (6).

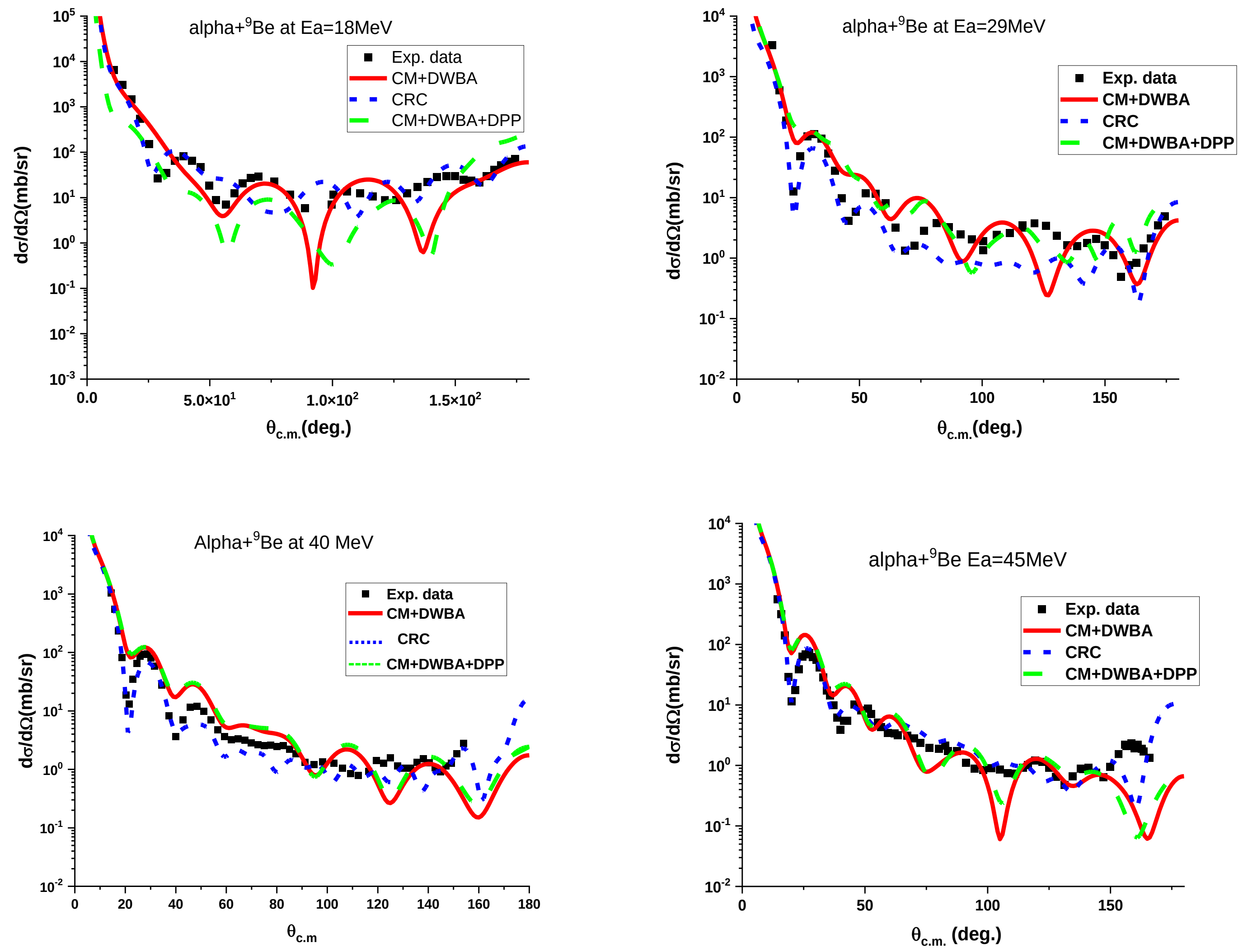

Fig. (5): Angular distribution for alpha elastically scattered by ^{9}Be, square dots represents experimental data, short dot lines (blue) represent CRC calculations and solid lines red lines represent calculated results from crystal model (CM+DWBA) and green lines are the CM+DWBA+DPP potential where experimental data were taken from [1-5].

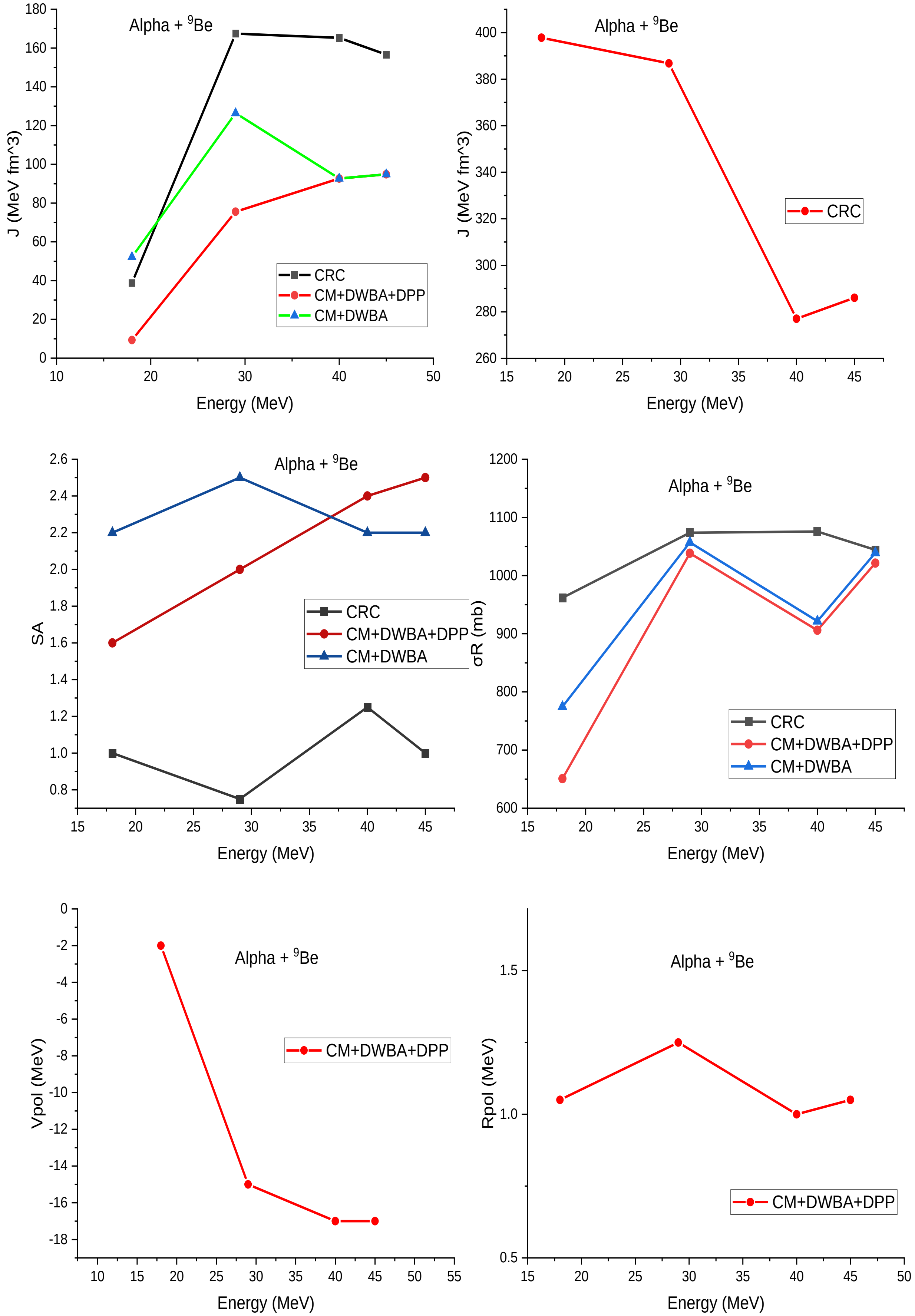

Alpha + 9Be
J (MeV fm^3)
Energy (MeV)
CRC
CM+DWBA+DPP
CM+DWBA
Alpha + 9Be
J (MeV fm^3)
Energy (MeV)
CRC
Alpha + 9Be
SA
Energy (MeV)
CRC
CM+DWBA+DPP
CM+DWBA
Alpha + 9Be
σR (mb)
Energy (MeV)
CRC
CM+DWBA+DPP
CM+DWBA
Alpha + 9Be
Vpol (MeV)
Energy (MeV)
CM+DWBA+DPP
Alpha + 9Be
Rpol (MeV)
Energy (MeV)
CM+DWBA+DPP

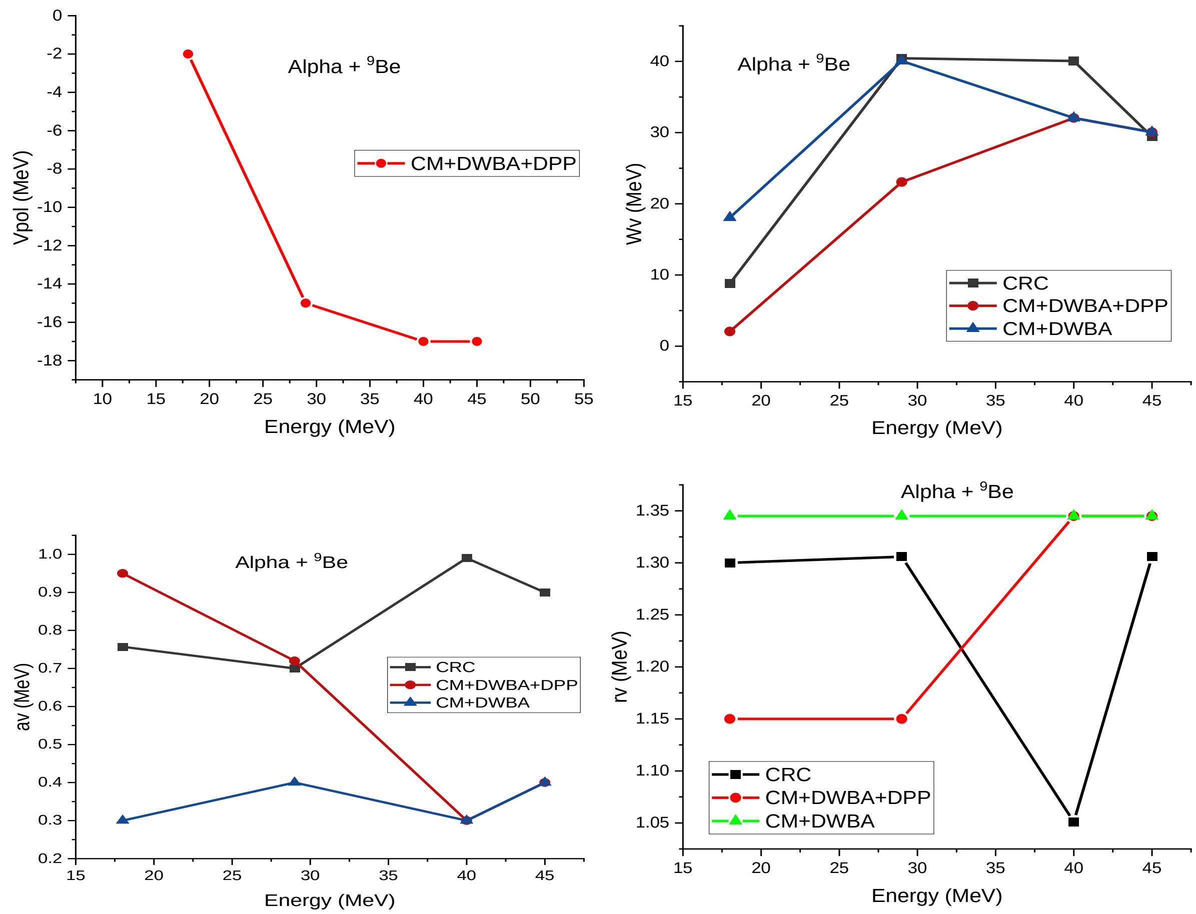

Fig. (6): Energy dependence of the total cross-section, real and imaginary potentials, DPP parameters, SA, radius, diffuseness, and volume integrals for the real and imaginary parts of the CM+DWBA and CM+DWBA+DPP potentials per nucleon pair for α-particles elastically scattered by ^{9}Be

Table (4): The parameters obtained for alpha elastically scattering by ^{9}Be with fixed r_c at 1.3 fm for calculations where (CM) is crystal model calculations

E_α MeV	Model	V_0, MeV	r_0, fm	a_0, fm	W_v, MeV	r_v, fm	a_v, fm	$V_{pol.}$	$r_{pol.}$	$a_{pol.}$	J_v MeV.fm^3	J_w MeV.fm^3	SA	σ_R, mb	Ref.
18.0	CRC	98.8	1.45	0.8	08.8	1.30	0.757				397.8	38.76	1.00	961.87	[22]
	CM+DWBA+DPP		Nr=0.9		02.06	1.150	0.95	-2.0	1.05	0.65		9.319	1.60	650.70	
	CM+DWBA		Nr=1.0		18.06	1.345	0.30					52.19	2.20	774.51	
29.0	CRC	095.0	1.45	0.80	40.44	1.306	0.70				386.8	167.42	0.75	1073.6	[22]
	CM+DWBA+DPP		Nr=0.7		23.06	1.150	0.72	-15.0	1.25	0.65		75.555	2.00	1038.4	
	CM+DWBA		Nr=1.0		40.06	1.345	0.40					126.42	2.50	1057.0	
40.0	CRC	81.0	1.38	0.73	40.06	1.051	0.990				277.0	165.25	1.25	1075.7	[22]
	CM+DWBA+DPP		Nr=0.7		32.06	1.345	0.30	-17.0	1.00	0.50		92.649	2.40	905.93	
	CM+DWBA		Nr=1.0		32.06	1.345	0.30					92.64	2.20	921.51	
45.0	CRC	79.0	1.45	0.73	29.44	1.306	0.90				286.0	156.63	1.00	1044.2	[22]
	CM+DWBA+DPP		Nr=0.70		30.06	1.345	0.40	-17.0	1.05	0.50		94.863	2.50	1021.35	
	CM+DWBA		Nr=1.0		30.06	1.345	0.40					94.86	2.20	1039.0	

3.4 Alpha Elastically scattered on ^{11}B

The analysis of alpha elastically scattered by ^{11}B at energies 29-65MeV [60-63] has been performed phenomenologically using (CRC) and semi-microscopically (CM). The effect of inelastic and ^{7}Li transfer has been studied as shown in Fig.(9). Woods-Saxon (WS) forms have been chosen to perform the present analysis for both real and imaginary parts of the potential where the radii $r_o = 1.281\,fm$ and $r_v = 1.34\,fm$. Also, CM has been applied to alpha elastically scattered by ^{11}B. Elastic, inelastic and ^{7}Li transfer with elastic scattering for alpha elastically scattered by ^{11}B has been involved in the fitting process to study the effect of inelastic and transfer on the elastic scattering. The fitting has been performed using four free parameters $\boldsymbol{W_V}$, $\boldsymbol{a_V}$, $\boldsymbol{N_r}$ and SA; for $^{11}B \equiv \alpha + ^{7}Li$ configuration. The imaginary part of the optical potential was taken from CRC as starting parameters for CM +DWBA calculations. DPP has been applied to alpha elastically scattered by ^{11}B as shown in Fig.(7).

The obtained optical parameters extracted from CRC method, CM+DWBA potential, and CM+DWBA+DPP potential values of the real (J_v) and the imaginary (J_w) volume integrals in addition to the values of the total reaction cross sections σ_R for the four studied energies under consideration are listed in Table (5). Spectroscopic amplitude for the ground state has been applied to the excited states because the research deals with the ground state of ^{11}B. Inelastic scattering has been achieved at the ground $1/2^-$ and first excited state $3/2^-$ of ^{11}B. For inelastic scattering, the deformation parameter β_2 was taken 0.92 with $\beta_\lambda R_V$=1.75fm for ^{11}B. CM+DWBA+DPP potential and CRC could reasonably reproduce the differential cross section in the whole range of the energies under consideration and angular range in spite of the CRC method still better than the modified potential (CM+DWBA+DPP). The real volume integral (J_v) decreases with energy increase where the imaginary volume integral (J_w), in a contrary with the real volume integral, is proportional to energy (see Table 5). The extracted ***SA*** values from CM+DWBA is nearly twice their values obtained from CRC calculations at the same incident energy for α+^{11}B system. CM+DWBA+DPP potential could not enhance the fitting process for α+^{11}B. It was noticed that, the obtained total reaction cross sections for α+^{11}B at energies 40–50MeV are not far off that calculated in [62] . The experimental data in the energy range under consideration offerings an airy minimum pattern for α +^{11}B nuclear system as shown in Fig. (7) where the positions of airy minimum pattern was observed with a shift to smaller angles in theforward angles when the energy of the projectile is increased.

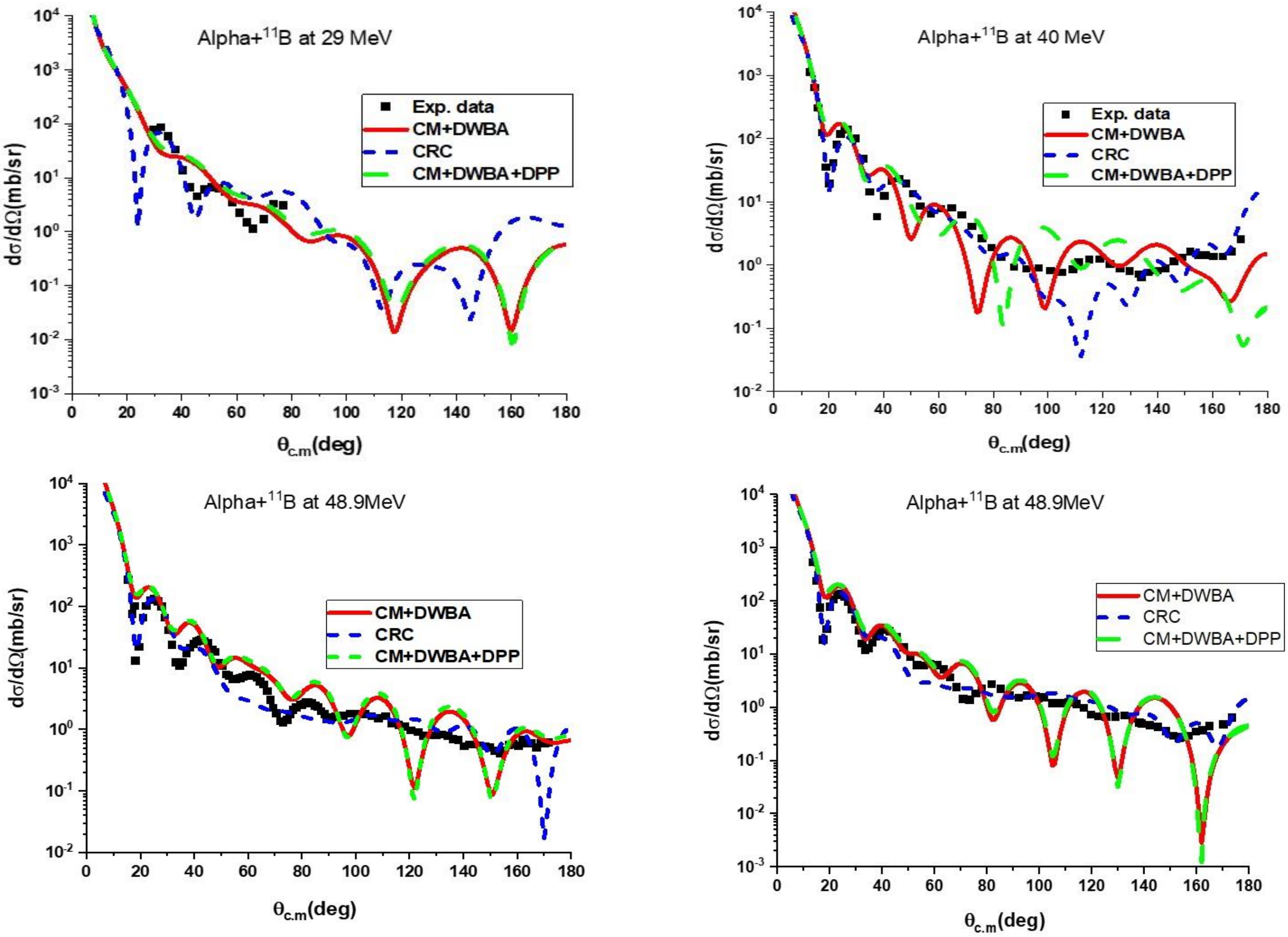

Fig. (7): Angular distribution for alpha elastically scattered by ^{11}B, short dot lines (blue) represent CRC calculations and solid lines red lines represent calculated results from crystal model (CM+DWBA) and green lines are the CM+DWBA+DPP potential re square dots represent experimental data, and lines represent calculated results from crystal model where experimental data were taken from [60-63].

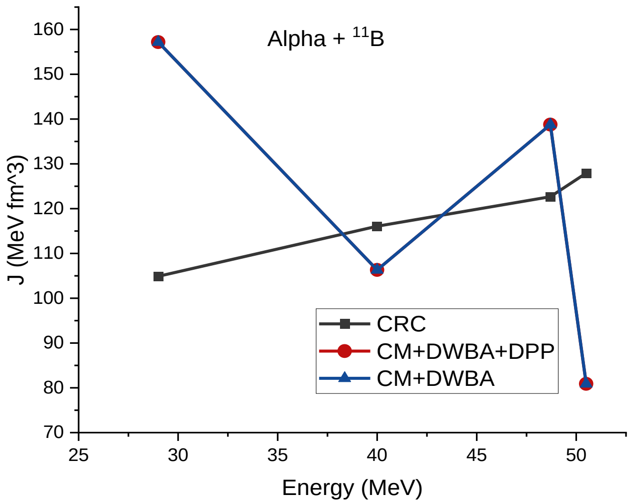
Alpha + ^{11}B
J (MeV fm^3)
Energy (MeV)
CRC
CM+DWBA+DPP
CM+DWBA

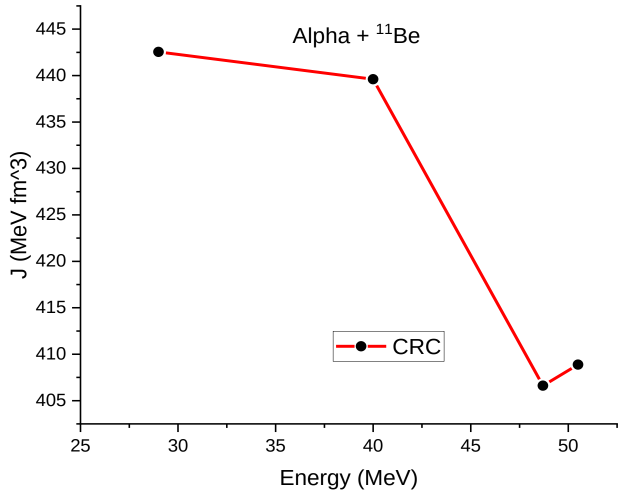
Alpha + ^{11}Be
J (MeV fm^3)
Energy (MeV)
CRC

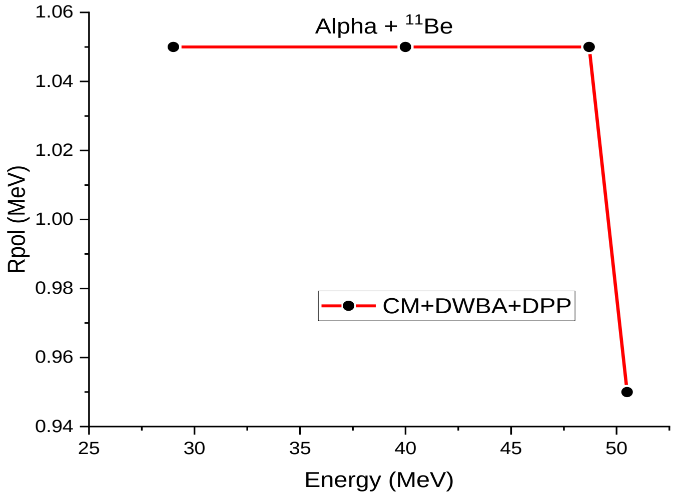
Alpha + ^{11}Be
Rpol (MeV)
Energy (MeV)
CM+DWBA+DPP

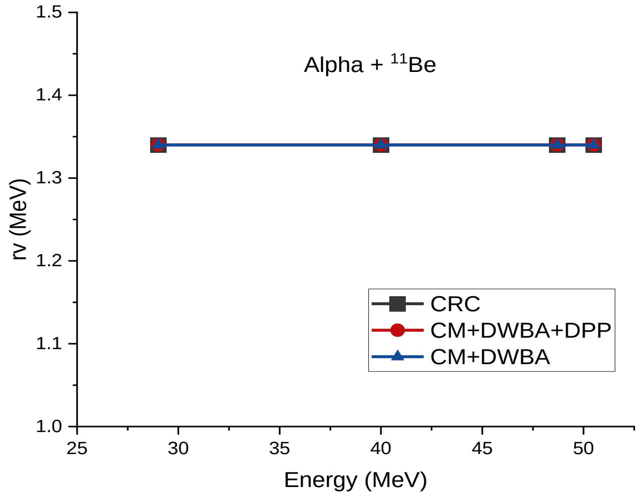
Alpha + ^{11}Be
rv (MeV)
Energy (MeV)
CRC
CM+DWBA+DPP
CM+DWBA

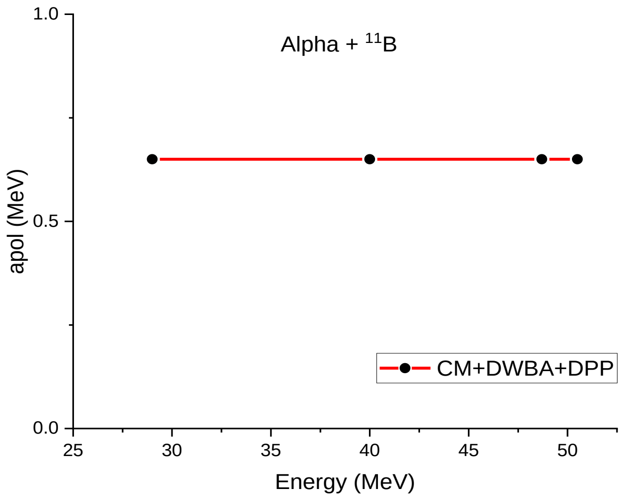
Alpha + ^{11}B
apol (MeV)
Energy (MeV)
CM+DWBA+DPP

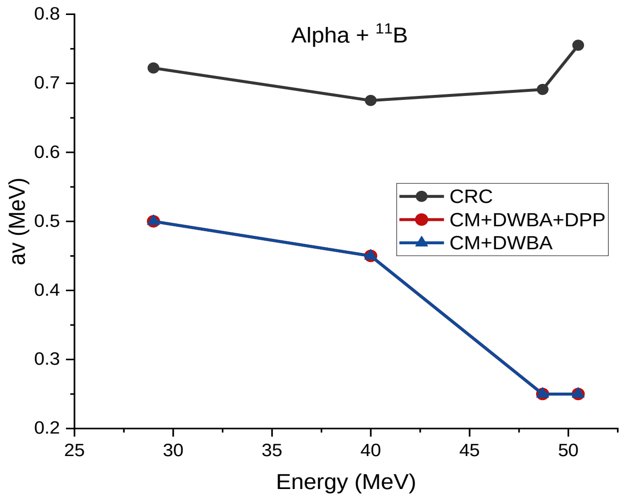
Alpha + ^{11}B
av (MeV)
Energy (MeV)
CRC
CM+DWBA+DPP
CM+DWBA

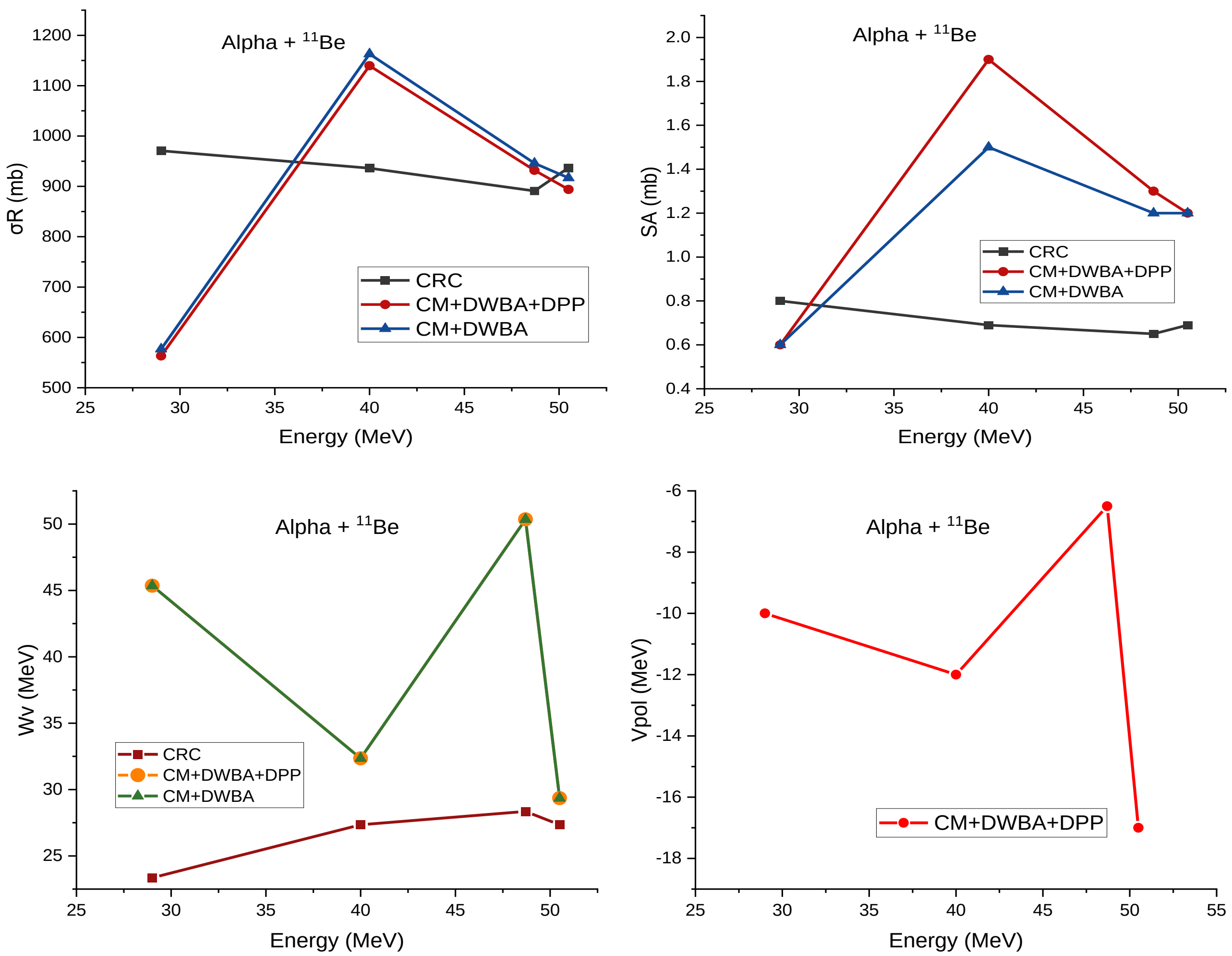

Fig. (8): Energy dependence of the total cross-section, real and imaginary potentials, DPP parameters, SA, radius, diffuseness, and volume integrals for the real and imaginary parts of the CM+DWBA and CM+DWBA+DPP potentials per nucleon pair for α-particles elastically scattered by ^{11}B

Table (5): The parameters obtained for alpha elastically scattering by ^{11}B with fixed r_c at 1.3 fm for calculations where (CM) is crystal model calculations

E_α MeV	Model	V_0, MeV	r_0, fm	a_0, fm	W_v, MeV	r_v, fm	a_v, fm	$V_{pol.}$	$r_{pol.}$	$a_{pol.}$	J_v MeV.fm^3	J_w MeV.fm^3	SA	*σ_R, mb*	*Ref.*
29	CRC	130.4	1.28	0.69	23.35	1.34	0.722				442.55	104.90	0.80	970.70	**[22]**
	CM+DWBA+DPP		Nr=1.0		45.35	1.340	0.50	-10.0	1.05	0.65		157.17	0.60	563.27	
	CM+DWBA		Nr=0.56		45.35	1.340	0.50					157.17	0.60	576.87	
40	CRC	126.4	1.28	0.73	27.35	1.34	0.675				439.60	116.07	0.69	936.20	**[22]**
	CM+DWBA+DPP		Nr=1.0		32.35	1.340	0.45	-12.0	1.05	0.65		106.30	1.90	1139.7	
	CM+DWBA		Nr=0.40		32.35	1.340	0.45					106.30	1.50	1162.9	
48.7	CRC	115.2	1.28	0.72	28.35	1.34	0.691				406.61	122.66	0.65	891.00	**[22]**
	CM+DWBA+DPP		Nr=1.0		50.35	1.340	0.25	-6.5	1.05	0.65		138.77	1.30	931.94	
	CM+DWBA		Nr=0.50		50.35	1.340	0.25					138.77	1.20	945.97	
50.5	CRC	114.4	1.28	0.73	27.35	1.34	0.755				408.88	127.91	0.69	937.00	**[22]**
	CM+DWBA+DPP		Nr=1.0		29.35	1.340	0.25	-17.0	0.95	0.65		80.89	1.20	893.98	
	CM+DWBA		Nr=0.50		29.35	1.340	0.25					80.89	1.20	916.83	

3.5 Deuteron elastically scattered by ^{6}Li

In the case of the deuteron elastically scattered by light nuclei, only the attractive force between nucleons are considered, where no more than one proton inside the nucleus. The form of the potential between two nucleons suggested by the authors of the present study is taken as from Equation 2; $V_{CM}(R) = -V_0 \exp[-A(\frac{R}{r_0})^2]$, where A=2, V_0=28MeV and $(r_0)^2$=0.81fm; A is the atomic number of the deuteron. The parameters obtained for deuteron elastically scattering by ^{6}Li is given in Table (6). CM+DWBA potential has been suggested by us to analyze the experimental data for deuteron elastically scattered by $^{6,7}Li$. The fitting of the experimental data for deuteron elastically scattering by ^{6}Li using CM+DWBA potential and CM+DWBA+DPP potential is given in Fig. (9).

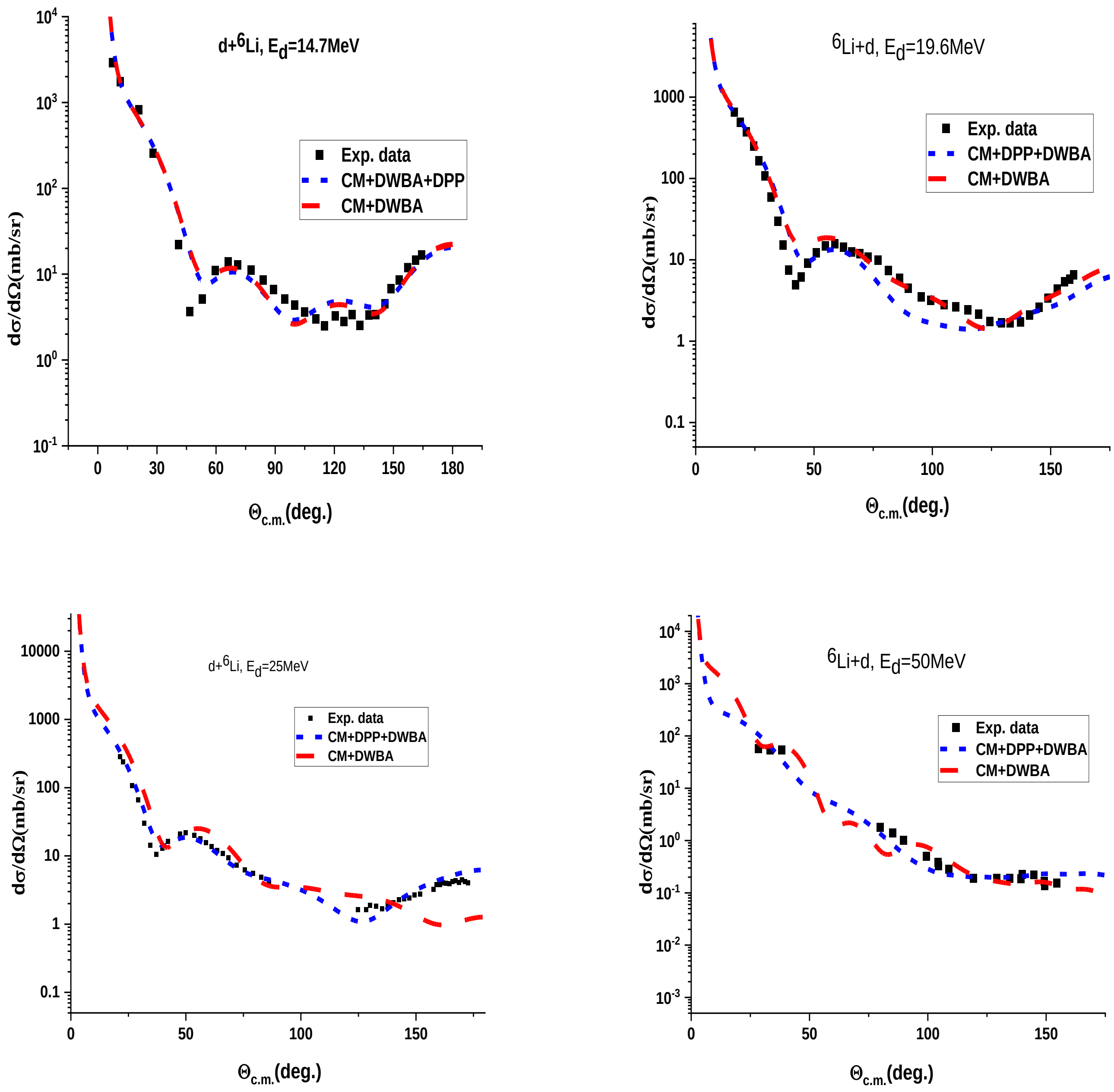

Fig. (9): Angular distribution for deuteron elastically scattered by ^{6}Li, square dots represents experimental data, short dot lines (blue) represent CM+DWBA+DPP calculations and red lines represent calculated results from CM+DWBA

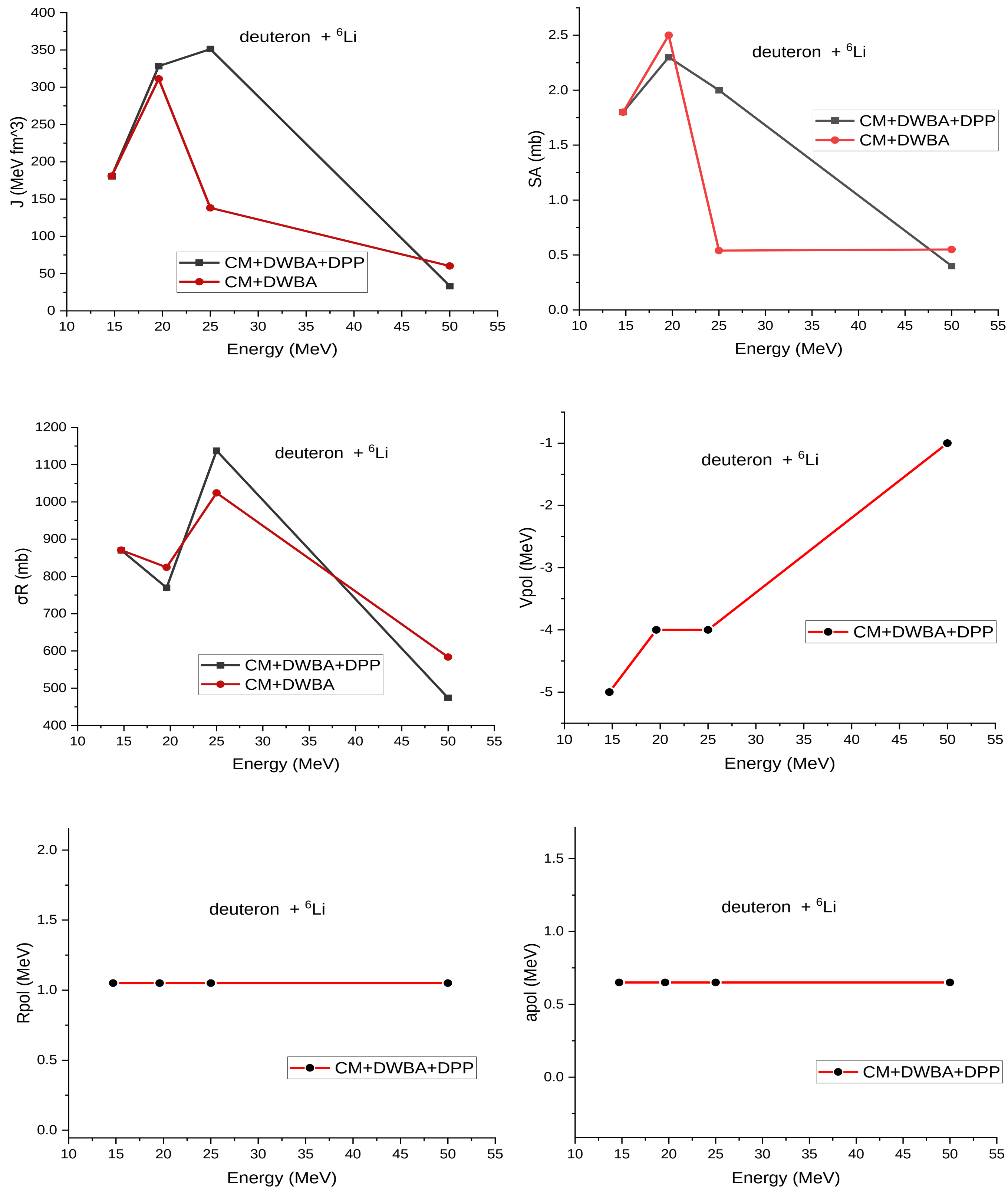

deuteron + 6Li
J (MeV fm^3)
Energy (MeV)
CM+DWBA+DPP
CM+DWBA
deuteron + 6Li
SA (mb)
Energy (MeV)
CM+DWBA+DPP
CM+DWBA
deuteron + 6Li
σR (mb)
Energy (MeV)
CM+DWBA+DPP
CM+DWBA
deuteron + 6Li
Vpol (MeV)
Energy (MeV)
CM+DWBA+DPP
deuteron + 6Li
Rpol (MeV)
Energy (MeV)
CM+DWBA+DPP
deuteron + 6Li
apol (MeV)
Energy (MeV)
CM+DWBA+DPP

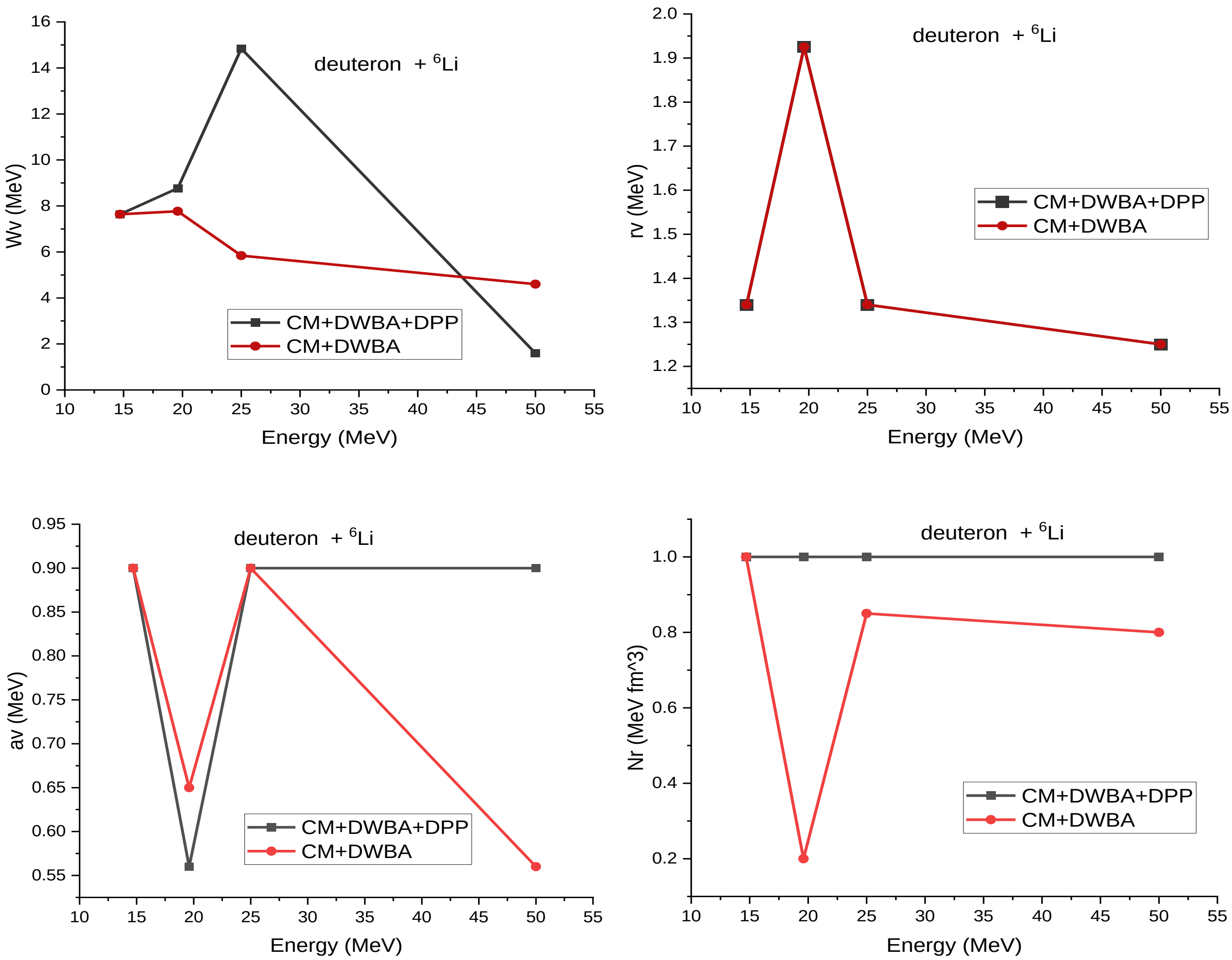

Fig. (10): Energy dependence of the total cross-section, real and imaginary potentials, DPP parameters, SA, radius, diffuseness, and volume integrals for the real and imaginary parts of the CM+DWBA and CM+DWBA+DPP potentials per nucleon pair for deuteron elastically scattered by ^{6}Li

Table (6): The parameters obtained for deuteron elastically scattering by ^{6}Li with fixed r_c at 1.3 fm for calculations where (CM) is the crystal model calculations

E_α MeV	Model	*Nr*	W_v, MeV	r_v, fm	a_v, fm	$V_{pol.}$	$r_{pol.}$	$a_{pol.}$	J_w MeV.fm^3	SA	σ_R, *mb*
14.7	CM+DWBA	1.0	07.64	1.340	0.90				180.82	1.8	870.72
	CM+DWBA+DPP	1.0	07.64	1.340	0.90	-5.0	1.05	0.65	180.82	1.8	870.72
19.6	CM+DWBA	0.2	07.77	1.925	0.65				311.29	2.5	824.42
	CM+DWBA+DPP	1.0	08.77	1.925	0.56	-4.0	1.05	0.65	328.33	2.3	769.68
25	CM+DWBA	0.85	05.84	1.340	0.90				138.22	0.54	1024.0
	CM+DWBA+DPP	1.0	14.84	1.340	0.900	-4.0	1.05	0.65	351.23	2.0	1137.5
50	CM+DWBA	0.80	4.60	1.250	0.56				60.21	0.55	583.61
	CM+DWBA+DPP	1.0	1.60	1.250	0.90	-1.0	1.05	0.65	33.37	0.40	473.75

3.6 Deuteron elastically scattered by ^7Li

The deuteron elastic scattering by ^6Li has been done using crystal model potential where its role appears at the forward angles. The deuteron elastic scattering by ^6Li has been done using crystal model (CM+DWBA) potential in addition to CRC method. CM+DWBA+DPP potential has not improve the analysis at the lower energies where the spectroscopic amplitude of $^7Li \equiv ^2H + ^5He$ has been increased from 1.2 to 1.3 for compensating the absorption result from DPP at 14.7MeV (see Fig. 11). The analysis of the experimental data at 25 and 28MeV supports the idea of break-up of the target in spite of deuteron also, undergoes the break-up process where it has the lowest binding energy in the nuclear systems. The adding DPP enhanced the analysis very well at E_d=28MeV as shown in Fig. (11). The CM+DWBA potential could fit the data under consideration with Nr less unity where adding DPP potential enables us to use N_r equal the unity as given in Table (7).

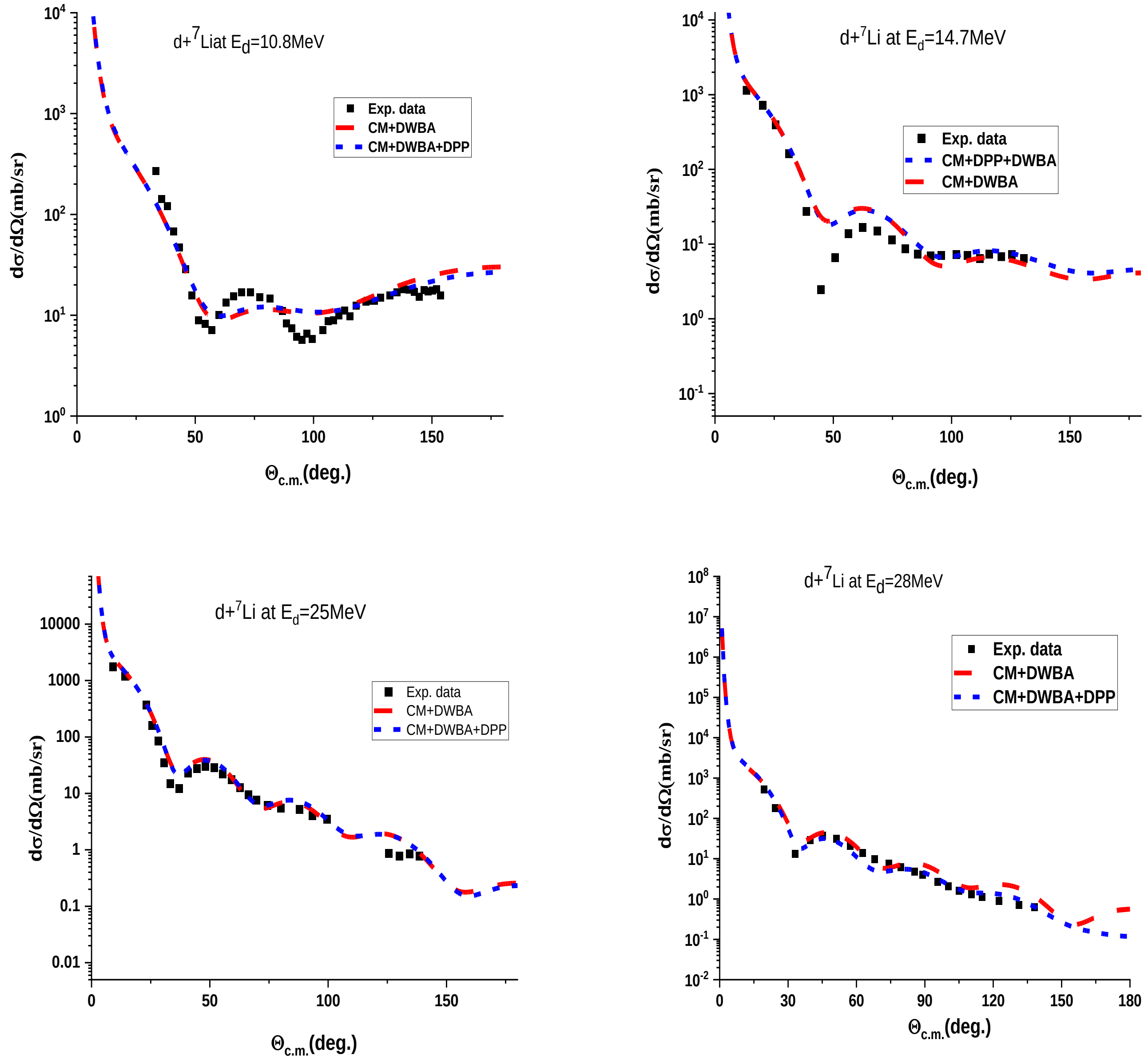

Fig. (11): Angular distribution for deuteron elastically scattered by ^7Li, square dots represents experimental data, short dot lines (blue) represent CM+DWBA+DPP calculations and red lines represent calculated results from CM+DWBA

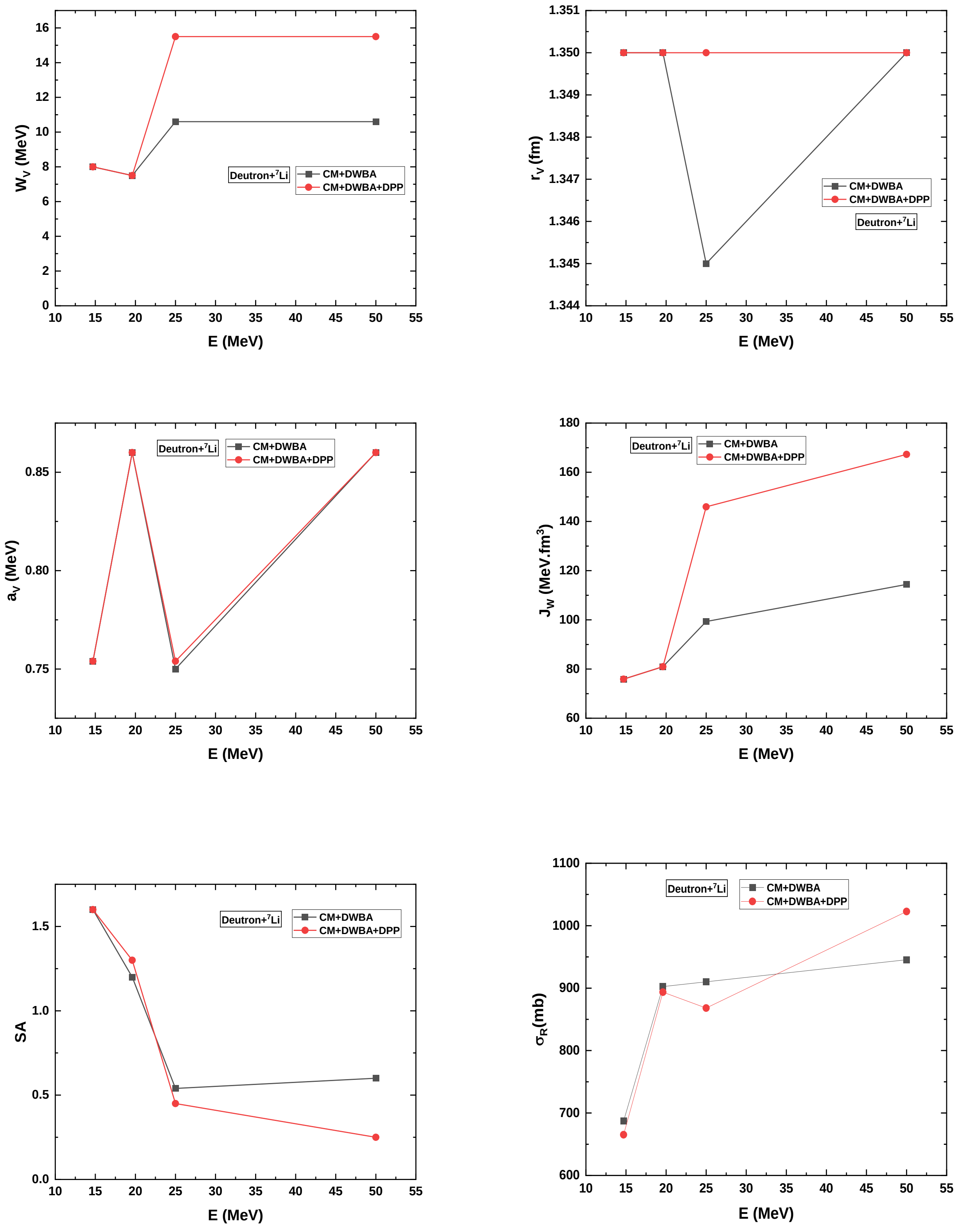
Deutron+7Li
CM+DWBA
CM+DWBA+DPP
WV (MeV)
E (MeV)
rV (fm)
E (MeV)
aV (MeV)
E (MeV)
JW (MeV.fm3)
E (MeV)
SA
E (MeV)
σR(mb)
E (MeV)

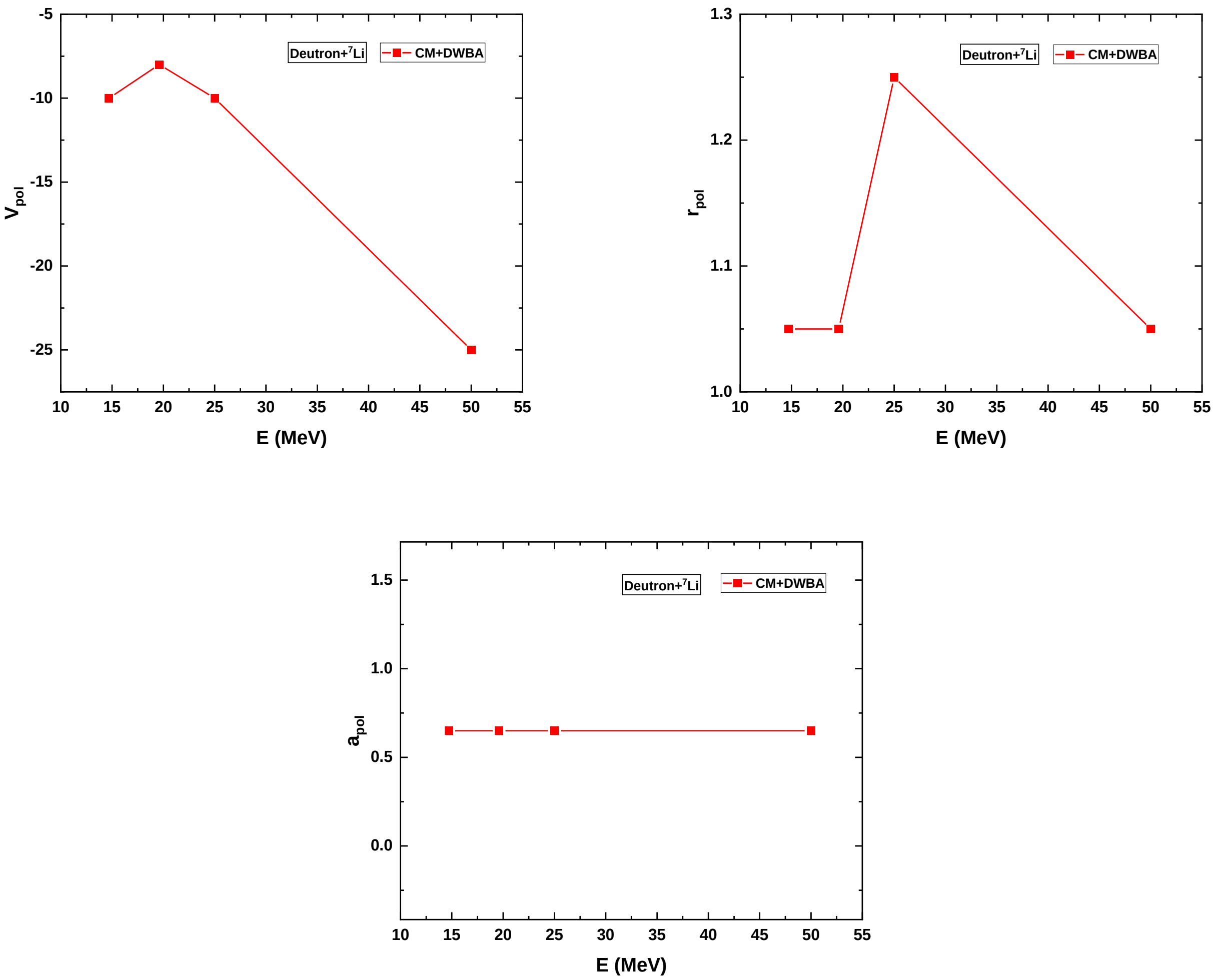

Fig. (12): Energy dependence of the total cross-section, real and imaginary potentials, DPP parameters, SA, radius, diffuseness, and volume integrals for the real and imaginary parts of the CM+DWBA and CM+DWBA+DPP potentials per nucleon pair for deuteron elastically scattered by ^{7}Li

Table (7): The parameters obtained for deuteron elastically scattering by ^{7}Li with fixed r_c at 1.3 fm for calculations where (CM) is crystal model calculations

E_α MeV	Model	*Nr*	W_v, MeV	r_v, fm	a_v, fm	$V_{pol.}$	$r_{pol.}$	$a_{pol.}$	J_w MeV.fm^3	SA	σ_R, *mb*
10.8	CM+DWBA	0.20	08.00	1.350	0.754				75.9031	1.6	687.21
	CM+DWBA+DPP	1.00	08.00	1.350	0.754	-10.0	1.05	0.65	75.9031	1.6	665.17
14.7	CM+DWBA	0.7	07.50	1.350	0.86				80.9383	1.2	902.43
	CM+DWBA+DPP	1.0	07.50	1.350	0.86	-8.0	1.05	0.65	80.9383	1.3	893.51
25	CM+DWBA	1.5	10.60	1.345	0.75				99.3124	0.54	910.18
	CM+DWBA+DPP	1.0	15.50	1.350	0.754	-10.0	1.25	0.65	145.9290	0.45	868.09
28	CM+DWBA	1.2	10.60	1.350	0.860				114.3927	0.60	945.52
	CM+DWBA+DPP	1.0	15.50	1.350	0.86	-25.0	1.05	0.65	167.2724	0.25	1022.8

3.7 ^{6}Li elastically scattered by ^{12}C

The previous sections of this research paper were concerned with light-light nuclei whereas this section is connected to light-intermediate nuclei. ^{6}Li elastically scattered by ^{12}C has been reanalyzed at energies (36, 50.6, 90, 99, 123.5, 156, 168.6, 210, 318 and 600) [64-74] by two different potentials namely CM+DWBA and CM+DWBA+DPP. The position of ^{6}Li in the middle between light and heavy nuclei gives it the interest to study. It is considered as weakly bound nucleus and two clusters configuration ^{3}He+^{3}H and d+^{4}He has been suggested. In the previous study [4], the authors of the present work have introduced the crystal model potential as a new potential to study ^{6}Li elastically scattered by ^{12}C and reliable analysis has been obtained. In the present work, modification has been done by adding DPP to the CM+DWBA potential to enhance the value of N_r for ^{6}Li elastically scattered by ^{12}C. The depth and diffusiveness of imaginary part were taken as variable parameters where the radius was fixed (Table 6). Elastic and ^{6}Li transfer with elastic scattering have been studied as shown in Fig. (9).

The effect of involving DPP arises at all energies under consideration and at the whole angular range (Fig.9). At higher energies 318 and 600MeV CM+DWBA+DPP potential failed to reproduce differential cross section where succeeded at lower energies as shown in Fig.(9). The failure of CM+DWBA+DPP potential at 318 and 600MeV shows decouple of transfer with elastic scattering at such energies. At lower energies, CM+DWBA+DPP potential could reproduce differential cross sections, where DPP overcome the break up problem at intermediate energies **[75, 76]**. As the transfer of ^{6}Li with elastic scattering and inelastic scattering are uncoupled with elastic scattering, so, the analysis has been done with CM +DPP only as given in Table (6).

The extracted spectroscopic amplitudes and normalization factors were found to be energy dependent (Table 8). The CM+DWBA+DPP potential overcome the unhappiness factor of N_r where it is used to be equal unity. The extracted spectroscopic amplitudes started by 2.4 at 36MeV and was decreased to about 0.4 at the higher energies. The drop on the spectroscopic amplitudes at higher energies results from the break-up of ^{6}Li (Table 8). The discrepancy between the experimental data and their corresponding theoretical calculations shown at Figs. (1 and 3) appears again in Fig. (13) which may be resulting from shortage on the modeling or inelastic scattering which did involve during calculations as mentioned before.

Table (8): Obtained parameters for ^{6}Li elastically scattered by^{12}C using CRC method and CM+DWBA+DPP potential where $r_R = 1.324\ fm$, $r_V = 1.534 fm$, and $r_C = 1.3 fm$

E^{6}Li, MeV	**Model**	N_r	W_V, MeV	a_V, fm	$V_{pol.}$	$r_{pol.}$	$a_{pol.}$	J_W, MeV. fm^3	σ_R, mb	SA	**Ref.**
36	CM+DWBA	1.00	10.022	1.505				71.0141	1621	3	**[22]**
	CM+DWBA+DPP	1.00	10.022	1.505	-4.0	1.25	0.65	71.0141	1618	2.4	p.w.
50.6	CM+DWBA	0.30	27.02	0.870				109.335	1095	2	**[22]**
	CM+DWBA+DPP	1.00	27.022	0.870	-45.0	1.25	0.65	109.335	1066	1.8	p.w.
90	CM+DWBA	0.55	27.022	0.870				109.344	1608	2.2	**[22]**
	CM+DWBA+DPP	1.00	32.022	1.124	-60.0	1.25	0.65	142.1278	1453	1.0	p.w.
99	CM	0.37	31.241	1.052				148.439	1251	1.0	**[22]**
	CM+DWBA+DPP	1.00	52.241	1.400	-85.0	1.25	0.65	317.7525	2471	0.5	p.w.
123.5	CM	0.40	21.241	0.869				85.8768	889.9	1.0	**[22]**
	CM+DWBA+DPP	1.00	32.241	1.34	-75.0	1.25	0.65	182.7388	1741	1.0	p.w.
156	CM	0.50	52.641	0.864				211.907	1217	1.0	**[22]**
	CM+DWBA+DPP	1.00	34.641	0.865	-60.0	1.25	0.65	104.8240	1048	1.0	p.w.
168.6	CM	0.55	45.00	0.45				131.813	753.0	1.0	**[22]**
	CM+DWBA+DPP	1.00	30.00	0.865	-60.0	1.25	0.65	90.7803	980.0	1.0	p.w.
210	CM	0.20	65.00	0.45				190.397	684.7	0.7	**[22]**
	CM+DWBA+DPP	1.00	48.00	0.90	-90.0	1.25	0.65	152.9894	1169	1.0	p.w.
318	CM	0.42	56.00	0.56				176.573	748.6	1.0	**[2]**
	CM+DWBA+DPP	1.00	56.00	0.80	-90.0	1.25	0.65	153.3366	1007	0.4	p.w.
600	CM	0.65	45.55	0.65				153.620	729.4	1.0	**[22]**
	CM+ DPP	1.00	90.0	0.80	-120.0	1.25	0.65	246.4338	898.82	0.4	p.w.

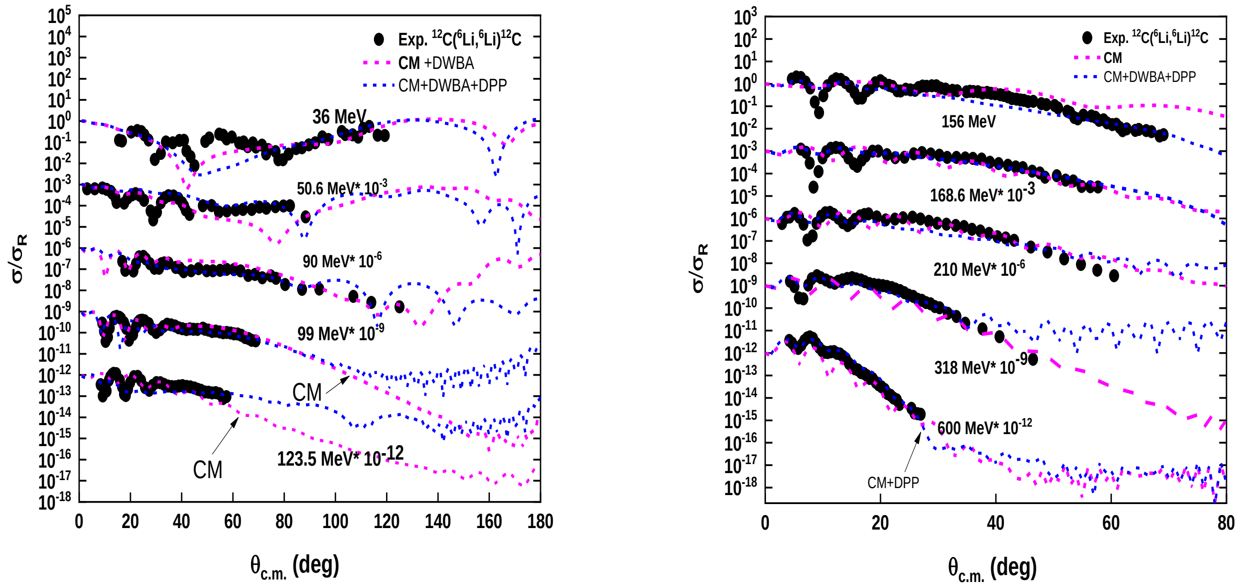

Fig. (13): ^{6}Li elastically scattered by ^{12}C at E_{lab} = (36, 50.6, 90, 99, 123.5, 156, 168.6, 210, 318 and 600). The solid circles are the experimental data where dash lines represent CM (magenta) with ^{6}Li transfer taken from [4] and short dash lines represent CM+DWBA+DPP (blue), except at 600MeV just CM+DPP

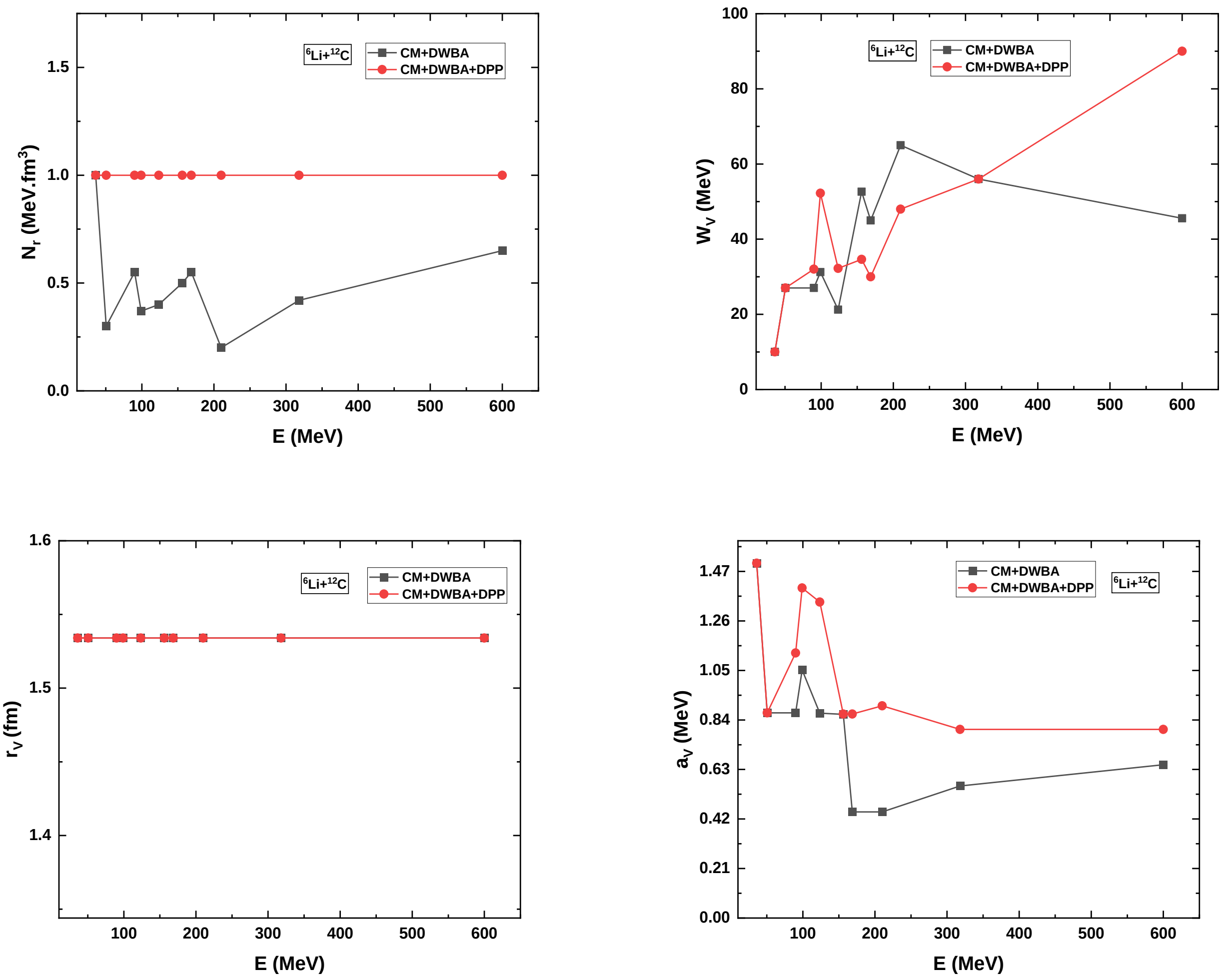

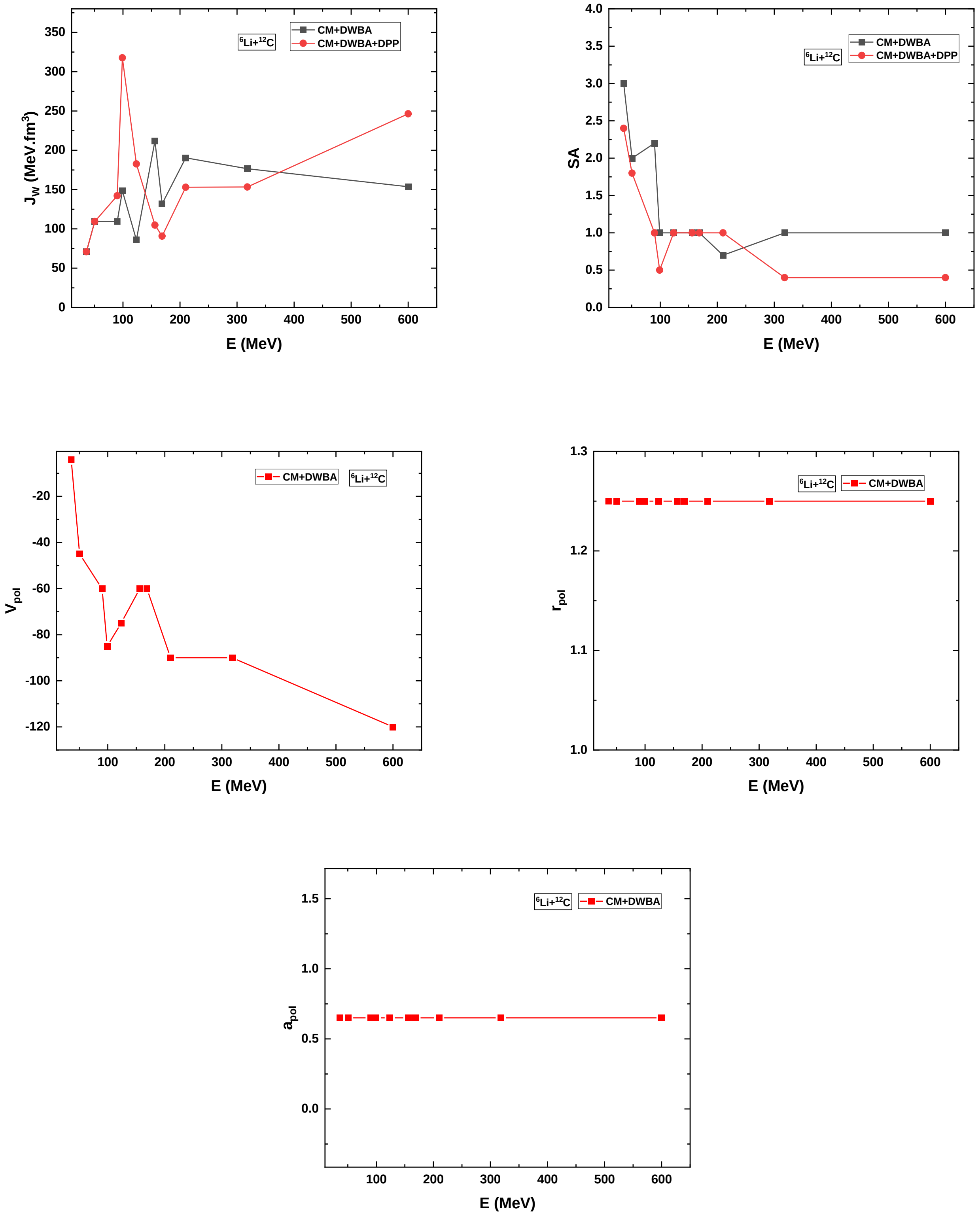

Fig. (14): Energy dependence of the total cross-section, real and imaginary potentials, DPP parameters, SA, radius, diffuseness, and volume integrals for the real and imaginary parts of the CM+DWBA and CM+DWBA+DPP potentials per nucleon pair for ^{6}Li elastically scattered by ^{12}C

CONCLUSIONS

The analysis of available experimental data has been done for alpha elastically scattering by light nuclei applying phenomenological and semi microscopic models. CRC method and CM+DWBA+DPP potential have been used to investigate the alpha elastic scattering on ^{6,7}Li, ^{9}Be and ^{11}B. CM+DWBA potential has been applied to the experimental data for analyzing the deuteron elastically scattered by ^{6,7}Li. The contribution of d, t, ^{5}He, and ^{7}Li transfer with elastic scattering for $\alpha + ^{6}$Li, $\alpha + ^{7}$Li, $\alpha + ^{9}$Be, and $\alpha + ^{11}$B, respectively has been observed at the backward angles. Extracting the optimal spectroscopic amplitudes has been done for all systems under consideration with different used potentials. The values of spectroscopic factors are extremely high at lower energies and decrease smoothly with energy increase. the aurhors believe that, the values of extracted spectroscopic factors at the higher energies is more reliable than those at lower energies. Adding DPP potential to CM+DWBA enhanced the analyses of the differential cross sections for all systems under consideration, especially for deuterons elastically scattered by ^{6,7}Li. The analysis of ^{6}Li elastically scattered by ^{12}C has been also carried out using CM+DWBA+DPP to interpret the break up process which takes place. The authors also concluded that the low binding energy of deuteron is responsible for break up process at deuterons elastically scattered by ^{6,7}Li. Non-normalized potential has been applied to all systems under consideration in the case of CM+DWBA+DPP potential. Poor analysis has been obtained for alpha elastic scattering by ^{9}Be and ^{11}B even using CM+DWBA+DPP potential. The crystal model (CM+DWBA), and (CM+DWBA+DPP) potentials succeeded to reproduce differential cross section at the whole angular range where coupled reaction channel (CRC) still the best choice between all applied models. The CM model was able to reproduce the differential cross section at lower energies than at relatively high energies for alpha elastic scattering on ^{6,7}Li, ^{9}Be and ^{11}B. Where for deuteron elastic scattering by ^{6,7}Li, CM succeeded to reproduce the differential cross section at all energies and at the whole angular range. It is observed that the calculated cross section (σ_R) behavior is energy dependent, potential dependent, the interacting nuclei dependent and could be accustomed by the normalization factor and spectroscopic amplitudes.

REFERENCES

[1] Y. A. Berezhnoy, V. YU. KORDA, and A. Gakh, "Matter-density distribution in deuteron and diffraction deuteron-nucleus interaction," J International Journal of Modern Physics E, vol. 14, no. 07, pp. 1073-1085, 2005.

[2] A. Amar and O. Hemeda, "Crystalline Model Approach for Studying the Nuclear Properties of Light Nuclei," International Journal of Nuclear and Quantum Engineering, vol. 15, no. 2, pp. 50-53, 2021.

[3] A. Amar, "Applying the Crystal Model Approach on Light Nuclei for Calculating Radii and Density Distribution," J International Journal of Nuclear Quantum Engineering, vol. 15, no. 12, pp. 217-222, 2022.

[4] A. Amar, A. M. El Mhlawy, A. Amer, and A. El Sayed, "Investigation the elastic scattering of isobar nuclei ^{6}Li and ^{6}He by ^{12}C using different nuclear potentials," J International Journal of Modern Physics E, p. 2250026, 2022.

[5] Ø. Jensen, G. Hagen, T. Papenbrock, D. J. Dean, and J. Vaagen, "Computation of spectroscopic factors with the coupled-cluster method," J Physical Review C, vol. 82, no. 1, p. 014310, 2010.

[6] G. Hagen and N. Michel, "Elastic proton scattering of medium mass nuclei from coupled-cluster theory," J Physical Review C, vol. 86, no. 2, p. 021602, 2012.

[7] P. Navratil, R. Roth, and S. Quaglioni, "Ab initio many-body calculation of the ^{7}Be(p, γ)^{8}B radiative capture," J Physics Letters B, vol. 704, no. 5, pp. 379-383, 2011.

[8] P. Navrátil and S. Quaglioni, "Ab Initio Many-Body Calculations of the ^{3}H(d,n)^{4}He and ^{3}He(d,p)^{4}He Fusion Reactions," J Physical Review Letters, vol. 108, no. 4, p. 042503, 2012.

[9] M. Lage, U.-G. Meißner, and A. Rusetsky, "A method to measure the antikaon–nucleon scattering length in lattice QCD," J Physics Letters B, vol. 681, no. 5, pp. 439-443, 2009.

[10] V. Bernard, M. Lage, U.-G. Meißner, and A. Rusetsky, "Scalar mesons in a finite volume," J

Journal of High Energy Physics, vol. 2011, no. 1, pp. 1-19, 2011.

[11] H. B. Meyer, "Photodisintegration of a Bound State on the Torus," arXiv preprint arXiv:1202.6675, 2012.

[12] R. A. Briceno and Z. Davoudi, "Moving multichannel systems in a finite volume with application to proton-proton fusion," J Physical Review D, vol. 88, no. 9, p. 094507, 2013.

[13] R. Guardiola, I. Moliner, and M. Nagarajan, "Alpha-cluster model for ^{8}Be and ^{12}C with correlated alpha particles," J Nuclear Physics A, vol. 679, no. 3-4, pp. 393-409, 2001.

[14] A. Amar, "Spectroscopic information of ^{6}Li from elastic scattering of deuterons, ^{3}He and ^{4}He by ^{6}Li," J International Journal of Modern Physics E, vol. 23, no. 08, p. 1450041, 2014.

[15] T. A. Lähde, E. Epelbaum, H. Krebs, D. Lee, U.-G. Meißner, and G. Rupak, "Lattice effective field theory for medium-mass nuclei," Physics Letters B, vol. 732, pp. 110-115, 2014.

[16] G. Rupak and D. Lee, "Radiative capture reactions in lattice effective field theory," Physical review letters, vol. 111, no. 3, p. 032502, 2013.

[17] U.-G. Meißner, "Clustering in nuclei from ab initio nuclear lattice simulations," arXiv preprint arXiv:1509.08290, 2015.

[18] Y. N. Eldyshev, V. Luk'yanov, And Y. S. Pol, "Analysis of elastic electron scattering on light nuclei on the basis of symmetrized fermi-density distribution," Joint Inst. For Nuclear Research, Dubna, Ussr1972.

[19] A. Tariq et al., "Potential description of anomalous large angle scattering of α particles," J Physical Review c, vol. 59, no. 5, p. 2558, 1999.

[20] A. Amar, "Analysis of Alpha Elastically Scattered by Light Nuclei Using Crystalline Model Approach," J Arab Journal of Nuclear SciencesApplications, vol. 55, no. 2, pp. 29-42, 2022.

[21] G. Satchler, "Nuclear Direct Reactions, Clarendon," vol. International series of monographs on physics (Oxford, England), ed. Oxford : Clarendon Press ; New York : Oxford University Press: Oxford, 1983.

[22] A. Amar, "Analysis of alpha elastically scattered by light nuclei applying different models," International Journal of modern physics E. vol. 31, no. 02, p. 2250011, 2022.

[23] V. Lapoux et al., "Coupling effects in the elastic scattering of ^{6}He on ^{12}C," Physical Review C, vol. 66, no. 3, p. 034608, 2002.

[24] H. Bohlen, N. Marquardt, W. Von Oertzen, and P. Gorodetzky, "Nucleon exchange in the low-energy scattering of α-particles on ^{6}Li and ^{7}Li," J. Nuclear Physics A, vol. 179, no. 2, pp. 504-512, 1972.

[25] H. Bingham, K. Kemper, and N. Fletcher, "Elastic scattering of ^{4}He from ^{6}Li and ^{7}Li at 12.0 to 18.5 MeV," J Nuclear Physics A, vol. 175, no. 2, pp. 374-384, 1971.

[26] S. Matsuki, S. Yamashita, K. Fukunaga, D. C. Nguyen, N. Fujiwara, and T. Yanabu, "Elastic and Inelastic Scattering of 14.7 MeV Deuterons and of 29.4 MeV Alpha-Particles by ^{6}Li and ^{7}Li," J Journal of the Physical Society of Japan, vol. 26, no. 6, pp. 1344-1353, 1969.

[27] V. Chuev, V. Davidov, B. Novatskii, A. Ogloblin, S. Sakuta, and D. Stepanov, "Elastic scattering of d, ^{3}He and α on ^{6}Li," J Le Journal de Physique Colloques, vol. 32, no. C6, pp. C6-163-C6-163, 1971.

[28] M. Bernas et al., "Anomaly in α-scattering from ^{6}Li between 35 and 45 MeV," J Nuclear Physics A, vol. 242, no. 1, pp. 149-159, 1975.

[29] V. Bragin et al., "Role of exchange effects in elastic scattering of α particles and ^{3}He ions by ^{6}Li nuclei," J Soviet Journal of Nuclear Physics, vol. 44, no. 2, pp. 198-203, 1986.

[30] N. Burtebaev, A. Duisebaev, B. Duisebaev, G. Ivanov, and S. Sakuta, "Elastic and inelastic scattering of 50-MeV alpha-particles by ^{6}Li and ^{7}Li nuclei: The role of exchange effects in anomalous scattering at large angles," J Physics of Atomic Nuclei, vol. 59, 1996.

[31] C. Samanta, S. Ghosh, M. Lahiri, S. Ray, and S. Banerjee, "Alpha-particle scattering from ^{6}Li near the α-d breakup threshold," J Physical Review C, vol. 45, no. 4, p. 1757, 1992.

[32] F. Foroughi, E. Bovet, and C. Nussbaum, "Elastic and inelastic scattering of alpha particles from ^{6}Li at 59 MeV" J Journal of Physics G: Nuclear Physics, vol. 5, no. 12, p. 1731, 1979.

[33] G. Hauser, R. Löhken, H. Rebel, G. Schatz, G. Schweimer, and J. Specht, "Elastic scattering of 104 MeV alpha particles" J Nuclear Physics A, vol. 128, no. 1, pp. 81-109, 1969.

[34] D. Bachelier et al., "Exchange effect in the 166 MeV α-particle elastic scattering on ^{6}Li" J Nuclear Physics A, vol. 195, no. 2, pp. 361-368, 1972.

[35] C. M. P. a. F. G. Pereyx. (January1976, 1). Atomic Data and Nuclear Data Tables.

[36] M. Nolte, H. Machner, and J. Bojowald, "Global optical potential for α particles with energies above 80 MeV" vol. 36, no. 4, p. 1312, 1987.

[37] X.-W. Su and Y.-L. Han, "Global optical model potential for alpha projectile" International Journal of Modern Physics E, vol. 24, no. 12, p. 1550092, 2015.

[38] S. Sakuta et al., "Role of channel coupling and deuteron-exchange mechanisms in anomalous alpha-particle scattering on ^{6}Li" J Physics of Atomic Nuclei, vol. 72, no. 12, pp. 1982-1991, 2009.

[39] U. Atzrott, P. Mohr, H. Abele, C. Hillenmayer, and G. Staudt, "Uniform α-nucleus potential in a wide range of masses and energies" J Physical Review C, vol. 53, no. 3, p. 1336, 1996.

[40] A. Kobos, B. Brown, R. Lindsay, and G. Satchler, "Folding-model analysis of elastic and inelastic α-particle scattering using a density-dependent force" J Nuclear Physics A, vol. 425, no. 2, pp. 205-232, 1984.

[41] H. Abele and G. Staudt, "α–^{16}O and α–^{15}N optical potentials in the range between 0 and 150 MeV," J Physical Review C, vol. 47, no. 2, p. 742, 1993.

[42] M.-E. Brandan and G. R. Satchler, "The interaction between light heavy-ions and what it tells us," J Physics reports, vol. 285, no. 4-5, pp. 143-243, 1997.

[43] O. Nemets and Y. V. Gofman, "Reference book on nuclear physics," 1975.

[44] K. Rusek, P. Cathers, E. Bartosz, N. Keeley, K. Kemper, and F. Marechal, "Scattering of polarized ^{7}Li from ^{4}He," J Physical Review C, vol. 67, no. 1, p. 014608, 2003.

[45] S. Matsuki, "Disintegration of ^{7}Li and ^{6}Li by 29.4 MeV Alhpa-Particles," J Journal of the Physical Society of Japan, vol. 24, no. 6, pp. 1203-1223, 1968.

[46] I. J. Thompson, "Fresco 2.0.," Department of physics,University of Surrey; Guildford GU2 7XH; England:, 2006.

[47] M. E.-A. Farid, A. A. Ibraheem, J. Al-Zahrani, W. Al-Harbi, and M. Hassanain, "Alpha-deuteron (triton) analysis of ^{6,7}Li elastic scattering," J Journal of Physics G: Nuclear Particle Physics, vol. 40, no. 7, p. 075108, 2013.

[48] S. Lukyanov et al., "Study of internal structures of ^{9,10}Be and ^{10}B in scattering of ^{4}He from ^{9}Be" J Journal of Physics G: Nuclear Particle Physics, vol. 41, no. 3, p. 035102, 2014.

[49] N. Burtebayev et al., "Elastic scattering of alpha particles from ^{9}Be in the framework of optical model," in Journal of Physics: Conference Series, 2020, vol. 1555, no. 1, p. 012032: IOP Publishing.

[50] S. Lukyanov et al., "Cluster Structure of ^{9}Be from ^{3}He+ ^{9}Be Reaction," in Journal of Physics: Conference Series, 2016, vol. 724, no. 1, p. 012031: IOP Publishing.

[51] S. Roy, J. Chatterjee, H. Majumdar, S. Datta, S. Banerjee, and S. Chintalapudi, "Coupled channel folding model description of α-scattering from ^{9}Be" J Physical Review C, vol. 52, no. 3, p. 1524, 1995.

[52] D. Janseitov et al., "Investigation of the elastic and inelastic scattering of ^{3}He from ^{9}Be in the energy range 30–60 MeV" J International Journal of Modern Physics E, vol. 27, no. 10, p. 1850089, 2018.

[53] B. Urazbekov et al., "Clusterization and strong coupled-channels effects in deuteron interaction with ^{9}Be nuclei" J Journal of Physics G: Nuclear Particle Physics, vol. 46, no. 10, p. 105110, 2019.

[54] K. Arai, P. Descouvemont, D. Baye, and W. Catford, "Resonance structure of ^{9}Be and ^{9}B in a

microscopic cluster model," J Physical Review C, vol. 68, no. 1, p. 014310, 2003.

[55] R. Peterson, "Alpha-particle scattering from ^{9}Be," J Nuclear Physics A, vol. 377, no. 1, pp. 41-52, 1982.

[56] R. Taylor, N. Fletcher, and R. Davis, "Elastic scattering of 4–20 MeV alpha particles by ^{9}Be," J Nuclear Physics, vol. 65, no. 2, pp. 318-328, 1965.

[57] A. Denikin et al., "Inelastic scattering and clusters transfer in ^{3,4}He+ ^{9}Be reactions," J Physics of Particles Nuclei Letters, vol. 12, no. 5, pp. 703-712, 2015.

[58] B. Lucas, S. Cosper, and O. Johnson, "Scattering of 18.4-MeV Alpha Particles by Beryllium," J Physical Review, vol. 133, no. 4B, p. B963, 1964.

[59] A. S. Demyanova et al., "Neutron halo in the exotic first excited state of ^{9}Be," J JETP letters, vol. 102, no. 7, pp. 413-416, 2015.

[60] N. B. e. al, "Investigation of the elastic and inelastic scattering of ^{4}He from ^{11}B in the energy range 29-50.5 MeV," Journal of Physics: Conference Series, vol. Ser. 940 012034, 2017.

[61] M. B. N Burtebaev, BA Duisebaev, RJ Peterson, SB Sakuta, "Scattering of α particles on ^{11}B nuclei at energies 40 and 50 MeV," J Physics of Atomic Nuclei, vol. 68 (8), no. (8), pp. 1303-1313, 2005.

[62] H. Abele et al., "Measurement and folding-potential analysis of the elastic α-scattering on light nuclei," J Zeitschrift für Physik A Atomic Nuclei, vol. 326, no. 4, pp. 373-381, 1987.

[63] A. Danilov et al., "Study of elastic and inelastic ^{11}B+α scattering and search for cluster states of enlarged radius in ^{11}B," J Physics of Atomic Nuclei, vol. 78, no. 6, pp. 777-793, 2015.

[64] K. Bethge, K. Meier-Ewert, and K. Pfeiffer, "Elastic scattering of ^{6}Li on ^{12}C at 20 MeV," Univ., Heidelberg, Zeitschrift für Physik1968, vol. 208.

[65] L. Chua, F. Becchetti, J. Jänecke, and F. J. N. P. A. Milder, "^{6}Li elastic scattering on ^{12}C, ^{16}O, ^{40}Ca, ^{58}Ni, ^{74}Ge, ^{124}Sn, ^{166}Er and ^{208}Pb at E (^{6}Li)= 50.6 MeV," vol. 273, no. 1, pp. 243-252, 1976.

[66] J. Cook, H. Gils, H. Rebel, Z. Majka, and H. J. N. P. A. Klewe-Nebenius, "Optical model studies of ^{6}Li elastic scattering at 156 MeV," vol. 388, no. 1, pp. 173-186, 1982.

[67] A. Dem'yanova et al., "Investigation of the nucleus-nucleus interaction at small distances in elastic scattering of ^{6}Li and the reaction (^{6}Li, ^{6}He) on carbon isotopes," vol. 501, no. 2, pp. 336-366, 1989.

[68] P. Kerr et al., "Tensor effects in ^{6}Li+ ^{12}C scattering," vol. 52, no. 4, p. 1924, 1995.

[69] A. Nadasen et al., "Elastic scattering of 210 MeV ^{6}Li ions from ^{12}C and ^{58}Ni and unique nucleus optical potentials," vol. 37, no. 1, p. 132, 1988.

[70] A. Nadasen et al., "Elastic scattering of 318 MeV ^{6}Li from ^{12}C and ^{28}Si: Unique phenomenological and folding-model potentials," vol. 47, no. 2, p. 674, 1993.

[71] J. E. Poling, E. Norbeck, and R. R. J. P. R. C. Carlson, "Elastic Scattering of Lithium by Carbon," vol. 5, no. 6, p. 1819, 1972.

[72] P. Schumacher, N. Ueta, H. Duhm, K.-I. Kubo, and W. J. N. P. A. Klages, "Lithium elastic and inelastic scattering and lithium-induced single nucleon transfer reactions," vol. 212, no. 3, pp. 573-599, 1973.

[73] P. Schwandt et al., "Optical potential for ^{6}Li elastic scattering at 99 MeV," vol. 24, no. 4, p. 1522, 1981.

[74] K. Schwarz et al., "Reaction mechanism of ^{6}Li scattering at 600 MeV," vol. 7, no. 3, pp. 367-375, 2000.

[75] H. Amakawa and K.-I. Kubo, "Spin-orbit potential in heavy-ion collisions," Nuclear Physics A, vol. 266, no. 2, pp. 521-532, 1976.

[76] Y. J. P. L. B. Sakuragi, "Breakup effect on ^{6}Li-nucleus scattering at intermediate energies," Physics Letters B, vol. 220, no. 1-2, pp. 22-26, 1989.